



Merz, Nina (2025) *Monitoring tidal hydrology within saltmarsh vegetation to detect current attenuation using the Mini Buoy*. MSc(R) thesis

<https://theses.gla.ac.uk/84871/>

Copyright and moral rights for this work are retained by the author

A copy can be downloaded for personal non-commercial research or study, without prior permission or charge

This work cannot be reproduced or quoted extensively from without first obtaining permission in writing from the author

The content must not be changed in any way or sold commercially in any format or medium without the formal permission of the author

When referring to this work, full bibliographic details including the author, title, awarding institution and date of the thesis must be given

Enlighten: Theses

<https://theses.gla.ac.uk/>  
[research-enlighten@glasgow.ac.uk](mailto:research-enlighten@glasgow.ac.uk)



# Monitoring tidal hydrology within saltmarsh vegetation to detect current attenuation using the Mini Buoy

NINA MERZ

Submitted in fulfilment of the requirements for the degree of

MSc (Res) Earth Science

School of Geographical and Earth Sciences

College of Science and Engineering

University of Glasgow

Supervisors: Dr. Alejandra G Vovides and Dr. Adrian Bass

## Abstract

Coastal zones are associated with growing populations, and with climate change increasing intensity and frequency of storms these communities are increasingly facing the threat of flooding. Saltmarshes are coastal ecosystems which are known to attenuate hydrodynamic energy thereby reducing risk for coastal populations. The incorporation of saltmarshes into coastal defence strategies is hindered by gaps in our knowledge concerning lateral saltmarsh dynamics and biophysical feedback networks. This knowledge is essential for accurately and reliably predicting the risk reduction capacity of nature-based solutions for flooding. Developing a tool for long-term hydrodynamic monitoring, quantifying the current velocity ( $C_v$ ) attenuation effects of salt marsh vegetation, and understanding how plant traits can impact the  $C_v$  attenuation capacity of saltmarsh species are critical steps towards better understanding saltmarsh dynamics.

In this study, we quantified the  $C_v$  attenuation of two salt marsh species (*Bolboschoenus maritimus* and *Phragmites australis*) that are abundant in the Inner Clyde Estuary. Using a novel low-cost method (the Mini-Buoy), we monitored hydrodynamics at the edge and five meters into the vegetation at three monospecific stands of each species. Two models of the Mini Buoy (the Pendant and the B4+) were compared against each other to determine which was better suited for deployment within saltmarsh vegetation and for quantifying current attenuation. Vegetation surveys at the start, middle, and end of the growing season (May-Sep) were carried out to associate plant traits with their attenuation effect. This study found that the Pendant Mini Buoy was the better model for hydrodynamic monitoring within the vegetation canopy and for quantification of current attenuation in shallow, low-energy conditions. Also, morphological adaptations to the physical environment were observed in both *B. maritimus* and *P. australis* where slenderness of the plants increased landward of the wave-exposed seaward boundary. Between the two species, significant differences in morphology and attenuation capacity were observed. Lower stem density and FSA was consistently observed in *P. australis* which was also found to develop in lower hydrodynamic energy areas, suggesting that *P. australis* is more vulnerable to hydrodynamic forcing. Overall, *B. maritimus* (maximum  $C_v$  reduction of ~60%) was found to be more effective at reducing current velocities than *P. australis* (maximum  $C_v$  reduction of ~40%).

## Acknowledgements

Thank you to Prof. Dr. Thorsten Balke for all the invaluable advice and feedback and for introducing me to this project and the GES and GALLANT teams, I've learned so much by being a part of this. Thank you to Dr. Alejandra G Vovides for all the Friday meetings, always being easily available to answer my questions, and for your unwavering support throughout this project. I'd also like to thank Dr. Adrian Bass for the feedback which was instrumental to the completion of this thesis.

A huge thank you to Kenny Roberts and Thomas Prentice for all the support in prepping the Mini Buoys and the muddy work of deploying them, I would have no data without your help. Thank you to Bachelor's student Clarissa and Master's students Xin and Yuning for their fieldwork support in conducting the plant trait assessments. Also, a huge thank you to Dr. Cai Ladd for all the help understanding the Mini Buoys and the Mini Buoy app.

Thank you to the whole GALLANT WP2 team - Dr. Dominic McCafferty, Dr. Davide Dominoni, Dr. Anna Bracken, Emma Plant, Jess Young, Will McGhee, and Ross Barnett – for their support and feedback on my work. You saw all my posters and presentations first and made them better; I learned so much from all of you.

Thank you to NatureScot for their interest in, and feedback on, this project and thank you to GALLANT (UKRI/NERC Ref. No. NE/W005042/1) for supporting this project.

Finally, thank you to my partner William Nibbs for all your support - you make me better. And to my family – Mami, Papi, Jana, Jaan - who have taken every step of this project alongside me and have supported me endlessly, a huge thank you and all my love.

# Contents

Abstract .....	2
Acknowledgements .....	3
Figures .....	6
Tables.....	7
1. Introduction.....	8
2. Literature Review .....	10
2.1. Saltmarshes .....	10
2.1.1. Saltmarsh Dynamics .....	12
2.1.2. Ecosystem Services.....	13
2.1.3. Anthropogenic impacts .....	15
2.2. Coastal defence .....	18
2.3. Hydrodynamic energy attenuation in saltmarshes.....	21
2.3.1. Benign conditions.....	21
2.3.2. Storm conditions.....	24
2.3.3. Impact of plant traits on attenuation capacity.....	25
2.4. Monitoring Coastal Hydrodynamics.....	26
2.4.1. The Mini Buoy.....	27
3. Methods.....	29
3.1. Field Site.....	29
3.2. Field Site Experimental Design .....	33
3.2.1. Effectiveness of two Mini Buoy models for the quantification of $C_v$ attenuation by vegetation.....	33
3.2.2. Assessment of plant traits for two saltmarsh species.....	35
3.2.3. Assessment in $C_v$ attenuation between two saltmarsh species.....	36
3.3. Statistical approach.....	36
3.3.1. Effectiveness of two Mini Buoy models for the quantification of $C_v$ attenuation by vegetation .....	36
3.3.2. Assessment of plant traits for two saltmarsh species.....	37
3.3.3. Assessing differences in $C_v$ attenuation between two saltmarsh species .....	37
4. Results .....	38
4.1. Inundation characteristics .....	38

4.1.1. Number of inundation events .....	38
4.1.2. Duration of inundation events .....	40
4.1.3. Number of inundation events with detectable currents .....	40
4.2. Assessment of vegetation traits .....	41
4.2.1. Slenderness .....	41
4.2.2. Stem density .....	41
4.2.3. Frontal surface area .....	42
4.3. Current velocity ( $C_v$ ) attenuation .....	43
4.3.1. Difference between species .....	43
4.3.2. Effect of plant traits on $C_v$ attenuation .....	46
5. Discussion .....	49
5.1. Effectiveness of two mini buoy models in quantifying $C_v$ attenuation inside vegetation	49
5.2. Plant traits of two saltmarsh species and their role in effective $C_v$ .....	51
5.3. Differences in current attenuation between two saltmarsh species .....	52
6. Conclusions .....	54
7. Bibliography .....	55

# Figures

Figure 1. Mini Buoys tethered to the ground. A) B4+ model of the Mini Buoy B) Pendant model of the Mini Buoy .....	28
Figure 2. Diagram of the placement of the rubber O-ring inside the lid of the centrifuge tube when assembling the B4+ Mini Buoy.....	29
Figure 3. Salt marsh distribution (green polygons) along the Inner Clyde Estuary Ramsar site (pink polygon). Source: map adapted from NatureScot (Haynes 2016).....	31
Figure 4. Layout of Mini Buoy logger deployment transects at the Dumbarton field site. Pendant and B4+ Mini Buoys were deployed 1m apart along each transect in parallel lines. ....	32
Figure 5. Train line through saltmarshes in the Inner Clyde Estuary at Dumbarton. ....	33
Figure 6. Representations of fully submerged B4+ and Pendant Mini Buoy models (figure adapted from Ladd et al. (2024)). ....	33
Figure 7. Boxplot depicting the number of inundation events recorded per day throughout the monitoring period by each Mini Buoy model at each logger position. A Wilcoxon test is used to compare the logger models. ....	39
Figure 8. Boxplots depicting the change in the slenderness of <i>B. maritimus</i> and <i>P. australis</i> , respectively, over the growing season. Mean plant slenderness on the mudflat and 5m into the vegetation is compared with the Wilcoxon test.....	41
Figure 9. Boxplots depicting the change in stem density of <i>B. maritimus</i> and <i>P. australis</i> over the growing season 5m into the vegetation. A) the change in mean stem density over time within each species respectively is compared with the Wilcoxon test. B) the mean stem densities of <i>B. maritimus</i> and <i>P. australis</i> over the growing season are compared to each other with the Wilcoxon test. ....	42
Figure 10. Boxplots depicting the change in frontal surface area of <i>B. maritimus</i> and <i>P. australis</i> over the growing season 5m into the vegetation. <b>A)</b> the change in mean frontal surface area over time within each species respectively is compared with the Wilcoxon test <b>B)</b> the mean frontal surface areas of <i>B. maritimus</i> and <i>P. australis</i> over the growing season are compared to each other with the Wilcoxon test. ....	43
Figure 11. Frequency of inundation events with detectable Cv (75th quantile value of inundation event greater than the HOBO logger detection limit) depicted as a percentage of all full inundation events detected across mudflat and vegetation logger positions for <i>B. maritimus</i> and <i>P. australis</i> respectively. ....	44
Figure 12. Cv reduction observed in <i>B. maritimus</i> and <i>P. australis</i> over the whole monitoring period compared using a Wilcoxon test.....	44
Figure 13. Cv reduction observed per month in <i>B. maritimus</i> and <i>P. australis</i> , respectively, compared using a Wilcoxon test. ....	45
Figure 14. Boxplots depicting the Cv reduction per species in response to initial Cv represented in inter-quartile bins. ....	46
Figure 15. Generalised additive model (GAM2) showing how current reduction (%) by two saltmarsh species, <i>B. maritimus</i> and <i>P. australis</i> , is impacted by <b>A)</b> stem density and <b>B)</b> initial Cv. Initial Cv, stem density, and sampling month were used as smoothing terms, logger transect and position as random effects, and species as a fixed effect. The solid lines represent fitted values while the envelopes represent the standard error. ....	48

# Tables

Table 1. Magnitudes of hydrodynamic energy attenuation by different saltmarsh species reported in published studies. ....	22
Table 2. Technical specifications for the HOBO UA-004-64 Pendant G and MSR145W B4 accelerometers. ....	35
Table 3. Cumulative number of days recorded throughout the monitoring period by each Mini Buoy model at each transect. ....	38
Table 4. Number of inundation events recorded throughout the monitoring period by each Mini Buoy model per species. ....	39
Table 5. Total inundation duration detected per species and logger position expressed as a percentage of the full duration of recording per logger. ....	40
Table 6. Inundation events with detectable currents expressed as a percentage of the total number of recorded inundation events (Table 4) per species and logger position. ....	40
Table 7. Summary of outcomes (deviance explained by the model and AIC) of three generalised additive models run on the HOBO data. ....	46



# 1. Introduction

Amongst several other essential ecosystem services, coastal habitats defend coastlines against flooding and erosion through the attenuation of wave energy reaching the shore (Möller et al. 2001; Barbier et al. 2011). This ecosystem service has been demonstrated by several coastal habitats globally including saltmarshes (Bouma et al. 2014) which are widespread along temperate coasts. Coastal areas are becoming increasingly exposed to natural hazards due to climate change and rising sea levels (Kaya et al. 2005; Wong et al. 2014) and traditional engineering coastal defence structures are proving unsustainable under these conditions due to the increased cost of upkeep (Temmerman et al. 2013). There is therefore an increasing interest in turning to nature-based solutions for coastal protection through the conservation, creation, and restoration of coastal habitats such as saltmarshes (Pétillon et al. 2023). However, the reliability of risk reduction estimates of nature-based solutions as coastal protection is dependent on detailed knowledge of the complex biophysical interactions that impact the hydrodynamic energy attenuation capacity of coastal ecosystems (Pétillon et al. 2023; Spalding et al. 2014; Temmerman et al. 2013). Though there have been growing contributions into this field of research in the past decade, there are still critical gaps in our knowledge about the physical thresholds of ecosystem-based coastal protection capacity.

Many factors including marsh topography, hydrodynamic conditions, and plant biophysical properties impact the attenuation capacity of a saltmarsh, and these factors can vary spatially and temporally (Leonardi et al. 2018). Having a detailed understanding of the impacts these biophysical properties have on attenuation capacity is essential to the assessment and implementation of nature-based coastal defences (Pétillon et al. 2023). Building this knowledge base requires the long-term collection of hydrodynamic, ecological, and sedimentological field data to contribute to more accurate and reliable modelling of ecosystem responses to hydrodynamic energy. A reliable, accessible method by which hydrodynamics can be measured at multiple spatial and temporal scales would therefore be a valuable resource to inform ecosystem-based management decisions.

Traditional hydrodynamic monitoring methods in the use of equipment such as tide gauges, velocimeters, and bottom mounted pressure sensors, are reliable but generally not the most time- or cost-effective methods for practical habitat management purposes. They are usually expensive and can require pre-existing infrastructure or specialist knowledge to operate. In contrast, the Mini Buoy has been presented as a lower cost, easy to transport, more highly accessible alternative that does not require specialist knowledge to utilise (Balke et al. 2021). The Mini Buoy contains an acceleration data logger which records acceleration along the Y-axis ( $Y_{acc}$ ) as G-forces ( $g$ ). From this acceleration data, the Mini Buoy can measure inundation, current velocities, and wave orbital velocities (Ladd et al., 2024). The Mini Buoy is an open-source tool for which the components are commercially available globally. It has been deployed before on mudflats and at the fringes of intertidal mangroves and salt marshes. In this study, the Mini Buoys were deployed at

the intertidal saltmarshes of the Inner Clyde Estuary, Scotland.

The Clyde Estuary is the largest on Scotland's west coast and has a history of heavy industry and urbanisation due to its association with the city of Glasgow. The environment of the River Clyde has historically been subject to anthropogenic pressures from trade, heavy industry, and human settlement on its banks that persist today as Glasgow's population continues to grow (World Population Review 2024). Direct anthropogenic actions including continuous dredging for shipping, pollution, and the implementation of embankments and seawalls as flood defences have altered the Clyde Estuary's natural hydrodynamic and sedimentological regimes (Karunarathna 2011). These alterations to, and the pollution of, the physical environment of the Inner Clyde Estuary threatens its intertidal habitats, including tidal flats and saltmarsh (Karunarathna 2011). The value of these natural habitats is recognised by its designation as a Ramsar wetland, a European Commission (EC) Special Protection Area, and a Site of Special Scientific Interest (Inverclyde Council 2019). The health of these habitats is essential to maintaining ecosystem services that benefit the socio-economic wellbeing of the city of Glasgow. Key amongst the ecosystem services that saltmarshes provide is their hydrodynamic energy attenuation capacity (Möller & Spencer 2002; Temmerman et al. 2013).

Damage associated with flooding in the Clyde Estuary averages £0.5 million per year (Kaya et al. 2005). The issue of flood management and prevention in this area will only become more critical as sea levels rise and climate change projections predict larger, more intense storms (Otto et al. 2018; Rennie & Hansom 2011). As the city of Glasgow takes steps towards implementing sustainable solutions throughout the city to deliver the priorities of the UN sustainable development goals (i.e., through city-university partnerships such as GALLANT – Glasgow as A Living Lab Accelerating Novel Transformation (GALLANT 2024)), the saltmarshes that persist on the banks of the Clyde could present an opportunity for the implementation of nature-based mitigation and management measures for flooding. An estimated 41ha of saltmarsh (saline and brackish) can be found in the Inner Clyde Estuary (Haynes 2016). These stands of saltmarsh vegetation are widely distributed in the Clyde Estuary and are floristically diverse (Haynes 2016) but their biogeomorphology and hydrodynamic energy attenuation potential is currently understudied. Particularly, the direct quantification of current attenuation in the field by saltmarsh vegetation with a focus on how different species morphology can impact attenuation capacity is understudied. As saltmarsh species have differing characteristic traits such as stem density, height, and diameter, it is expected that they also vary in their attenuation capacity.

Using the Inner Clyde Estuary as a focal site, the aims of this study are threefold:

1. To compare the use of two models of the Mini Buoy (B4+ and Pendant) for quantifying current attenuation within saltmarsh vegetation
2. To assess plant and community characteristics of two saltmarsh species abundant on the Inner Clyde Estuary
3. To assess differences in current attenuation between two saltmarsh species (*Phragmites australis* and *Bolboschoenus maritimus*)

## 2. Literature Review

### 2.1. Saltmarshes

Saltmarshes are a vegetated transition zone between marine and terrestrial environments which occur globally along temperate coastlines (Mcowen et al. 2017). They develop in relatively sheltered tidal areas such as estuaries, embayments, and along tidal river channels which can influence the type of saltmarsh that develops (Dijkema 1987; Haynes 2016). They are built through interactions between tides and localised hydrodynamics, sediment flow, and vegetation growth (Fagherazzi et al. 2020; Townend et al. 2011). As such, saltmarshes are highly dynamic environments where vegetation communities are heavily influenced by, and influential towards, local physical processes such as sediment erosion and accretion (Fagherazzi et al. 2020).

Saltmarsh vegetation consists of halophytic plants which colonise the upper intertidal zone approximately between the mean high water of neap tides and the highest spring tides (Balke et al. 2016). Species composition of saltmarsh communities vary regionally according to environmental conditions and can be associated specifically with certain geomorphological types of saltmarshes (Haynes 2016). For example, back-barrier saltmarshes, which form parallel to the coastline because of tidal intrusion into sand dunes, are associated with a greater diversity of species and vegetation communities than other saltmarsh types due, in part, to their intermingling with sand dune vegetation communities (Haynes 2016). Estuarine saltmarshes, which form at the mouth of estuaries where salinity can vary greatly due to regular influxes of both saline- and fresh-water, are associated with the presence of brackish saltmarsh species (commonly *Phragmites australis* and *Bolboschoenus maritimus*) more so than other geomorphological types of saltmarshes (Haynes 2016).

Major estuaries in England and Wales house the greatest expanses of saltmarsh in Great Britain (Foster et al., 2013) but a large number of smaller communities can be found distributed along the Scottish coastline in firths, sea lochs, and bays (Haynes 2016). The estimated 7,703 ha of saltmarsh in Scotland accounts for ~9.21-16.5% of total saltmarsh extent in Great Britain (Foster et al. 2013; Haynes 2016; Mcowen et al. 2017). Estuarine

saltmarshes make up the greatest total extent of saltmarsh in Scotland and all the nation's larger, uniform saltmarshes are found in estuarine systems along the east coast or in the Solway firth in the south-west (Haynes, 2016; Haynes et al., 2017). Meanwhile, the west coast of Scotland hosts a high volume of smaller, complex saltmarsh communities (Haynes, 2016; Haynes et al., 2017) such as fringing saltmarshes that can be found along the banks of tidal rivers where estuaries narrow. Though they make up only a small proportion of saltmarsh extent in Scotland, this type of saltmarsh can be found throughout the country (Haynes, 2016) including the upper tidal reaches of the River Clyde (Hansom et al. 2017; Jones & Ahmed 2000; Taubert & Murphy 2012).

The Inner Clyde Estuary on the south-western coast of Scotland has many well-established saltmarsh communities along its banks totalling an estimated extent of 41 ha (Haynes 2016). Jones & Ahmed (2000) only identified two saltmarsh sites in the area, both on the south bank of the Clyde at Erskine Harbour and at Newshot Island. Since then, a more recent study has detailed a more comprehensive exploration of the distribution of saltmarsh habitats in the Inner Clyde Estuary (Hansom et al. 2017). Hansom et al. (2017) also found that Newshot Island and the South bank of the Clyde hosted saltmarsh communities though they report a continuous expanse of saltmarsh vegetation fringing the Clyde from Langbank to Erskine Bridge. Moreover, the northern bank of the Clyde was also found to host fringing saltmarsh in fragmented communities from Dumbarton Castle to the Erskine Bridge (Hansom et al. 2017).

In the Inner Clyde Estuary, 43.9% (18ha) of the total saltmarsh extent is currently made up of brackish vegetation communities with an abundance of *Bolboschoenus maritimus* and *Phragmites australis* (Haynes 2016), the focal species in this study. The main distinction between saline and brackish saltmarshes are the levels of salinity in the intertidal habitats they occupy. Brackish saltmarshes occur in areas with large influxes of freshwater and can indicate lower levels of salinity in the environment (Haynes 2016). In Scotland, brackish saltmarshes are expanding and even replacing saline saltmarshes in some areas (Haynes 2016) thereby becoming an increasingly prominent component of Scotland's coastal habitats. The following review of research on saltmarshes (Section 2.1) does not make a distinction between brackish and saline saltmarshes and species. This is in an effort to consider as much knowledge produced on saltmarshes as possible as far as it is relevant to this study.

Saltmarshes form a range of unique habitats that are widely protected by legislation (Inverclyde Council 2019). Saltmarsh communities are valued for the many ecosystem services they provide to ecological functioning and to human economic activities (Barbier et al. 2011). Coastal defence (Möller & Spencer 2002; Rupprecht et al. 2017), habitat provisioning for resident and transient wildlife (e.g. Whitfield 2017), and carbon sequestration (Mueller et al. 2019) are just a few examples of these ecosystem services. The role of saltmarshes in coastal defence is especially relevant to this study and will be expanded upon in sections 2.2 and 2.3. Though saltmarshes have previously been

overlooked in research and public awareness as compared to other coastal ecosystems such as mangroves and coral reefs (Duarte et al. 2008; Mcowen et al. 2017), the value they provide in associated ecosystem services is increasingly attracting attention. Improving and maintaining the provision of these services forms the foundation of the movement to protect saltmarshes (Barbier et al. 2011; Gedan et al. 2009).

### 2.1.1. Saltmarsh Dynamics

Saltmarshes exist in highly dynamic coastal environments and their survival is dependent upon a complex system of biotic and abiotic processes that drive their expansion and erosion. The biogeomorphodynamic feedback networks created by interactions between the morphology of the habitat, the hydrological characteristics of the area, sediment dynamics, and the ecology of the marsh itself comprise saltmarsh dynamics (Da Lio et al. 2013; Townend et al. 2011). The composition and structure of saltmarsh communities were traditionally considered to be controlled by physical conditions such as inundation characteristics, elevation, and salinity (Townend et al. 2011). However, there is now a growing body of evidence to suggest that ecological interactions within vegetated communities such as competition and facilitation are also important in determining saltmarsh vegetation structure (Da Lio et al. 2013).

Species composition and distribution in a saltmarsh is primarily decided by physical factors as saltmarsh plant species are adapted to specific optimal inundation, exposure, and elevation conditions (Boorman 2003; Da Lio et al. 2013). However, it is evident that vegetation communities can modify their physical surroundings to promote their own survival, and this can give rise to inter-specific competition, a key driver of ecological dynamics within the marsh (e.g. Morris 2006). For example, in some cases, a negative feedback cycle can be initiated wherein saltmarsh species modify their physical environment to better suit their own survival and create opportunities for other species to proliferate and outcompete the original (Townend et al. 2011). This can be observed in the case of pioneer species whose presence on the marsh creates shelter and elevation enough for more sensitive saltmarsh species to encroach and establish themselves (Bruno 2000).

Interactions between saltmarsh vegetation and the physical environment can impact the survival of the marsh itself. For example, saltmarsh vegetation can promote the growth of platforms by enhancing sediment deposition by as much as 50% (Friedrichs & Perry 2001). The formation and stability of platforms that vegetation can colonise is essential to saltmarsh survival. The slower flow of water over saltmarsh canopies due to current attenuation by the vegetation encourages sediment settlement and deposition and protects the platform from erosion (Friedrichs & Perry 2001; Neumeier & Amos 2006). In the case of certain species such as *Spartina alterniflora*, sediment is retained by the plants themselves on leaves and stems (Townend et al. 2011). By trapping deposited sediments in their root networks, vegetation can stabilise the marsh platform to buttress the saltmarsh against lateral erosion (De Battisti et al. 2019). The retention of deposited

sediments allows the marsh platform to grow vertically above the high tide mark creating conditions for the saltmarsh to further colonise it. This vertical accretion also increases the elevation of the marsh platform which can increase oxygen availability in the soil thereby promoting biomass production (Marani et al. 2006). Greater aboveground plant biomass can increase the velocity dampening effect on estuarine flows (Friedrichs & Perry 2001; Townend et al. 2011), which then further enhances sediment deposition in, and vertical accretion of, the marsh, forming a positive feedback loop. Greater biomass production can also form a self-imposed positive feedback cycle wherein sediment aeration through plant transpiration allows biomass production to increase, which enhances sediment aeration (Marani et al. 2006).

These biogeomorphodynamic feedback networks allow saltmarshes to adapt to, and survive in, their physical environment. They also allow saltmarshes to deliver ecosystem services such as coastal stabilisation and hydrodynamic energy attenuation. However, as anthropogenic pressures on saltmarshes grow globally (Gilby et al. 2021; Lotze et al. 2006; Moser et al. 2012), anthropogenic activities in proximity to saltmarsh sites (further explored in section 2.1.3) can greatly influence each of these key processes thereby having significant impacts on saltmarsh dynamics. To better incorporate nature-based solutions in coastal defence strategies and planning, the outcomes of these biogeomorphodynamic interactions need to be better understood and more reliably predicted.

### 2.1.2. Ecosystem Services

Saltmarshes provide a range of ecosystem services globally such as recreational opportunities, provision of food and building materials, and coastal protection and stabilisation (Barbier et al. 2011). As a highly productive ecosystem, saltmarshes are of disproportionately high economic value in relation to their lower global coverage (Costanza et al. 2008, 2014; Barbier et al. 2011; Himes-Cornell et al. 2018). Saltmarshes also hold and provide value beyond economic worth (Gramling & Hagelman 2005). However, despite their global significance, saltmarsh habitats are relatively understudied (Duarte et al. 2008) and increasingly threatened with degradation and habitat loss due to direct impacts from human activities and the impacts of anthropogenic climate change and sea level rise (Gilby et al. 2021; Moser et al. 2012). This jeopardizes the continued delivery of key ecosystem service; the maintenance of ecosystem service delivery is a key argument for the protection and restoration of saltmarshes (Adams et al. 2021). This section will provide an overview of key ecosystem services that saltmarshes provide. These services can be broadly categorised into cultural services, provisioning services, supporting services, and regulating services.

Despite their integral role in human and community wellbeing, the cultural services provided by saltmarshes have perhaps the least research dedicated to them of all saltmarsh ecosystem services (McKinley et al. 2020). Saltmarshes have a unique aesthetic value which can have a positive impact on human well-being (Hermes et al.

2018). Unique landscapes that are perceived to be beautiful can improve psychophysical wellbeing (Chang et al. 2008), promote physical activity and social interaction and bring about a sense of community (Abraham et al. 2010). Saltmarshes can also embody the heritage of communities and provide them with spiritual value and a sense of place (Gramling & Hagelman 2005). As such, these cultural services can sometimes be difficult to economically value as they come down to preference and therefore, local stakeholder perceptions are a critical element of determining the value of cultural services provided by saltmarshes (McKinley et al. 2020; Zoderer et al. 2019). Furthermore, saltmarshes also provide opportunities for recreation, education, and tourism activities which can have great positive impacts on human well-being, especially at a local scale (Rendón et al. 2019). These activities include fishing, hunting, birdwatching, and walking all of which contribute to the local economy (Barbier et al. 2011; Himes-Cornell et al. 2018).

Many recreational opportunities in saltmarshes are underpinned by the plant and animal biodiversity this habitat supports which also provisions local human populations with food and other materials for consumption. One of the most common provisioning services that saltmarsh plants provide are as fodder for livestock (Knottnerus 2005). Saltmarsh plants including *Phragmites australis* and *Spartina patens* are harvested for bedding and winter fodder and are directly grazed by livestock (Kiviat & Hamilton 2001; Knottnerus 2005; Köbbing et al. 2013). *Phragmites australis* has also been utilised by humans globally for fuel by burning or the production of biogas, for construction as thatch for roofs and in walls for insulation, and for making a range of everyday objects such as musical instruments and mats for sleeping on (Kiviat & Hamilton 2001; Köbbing et al. 2013).

Saltmarsh vegetation is also a source of food for human consumption both directly and indirectly. Vegetation from saltmarshes such as several *Salicornia* species can be harvested and consumed as vegetables (Ríos et al. 2020). Indirectly, saltmarsh vegetation provides an essential source of protein to coastal populations by creating a habitat and nursery for marine invertebrate species (Whitfield 2017). These environments have been used by coastal populations for subsistence fishing activities including the harvesting of fish and shellfish directly from the marsh (Costa et al. 2001; Knottnerus 2005). The role of saltmarshes as nursery grounds for shellfish and a diversity of fish and crustacean species supports both subsistence and commercial fishing activities which benefit local economies (Barbier et al. 2011; Castagno 2018; Costa et al. 2001; Whitfield 2017). The shallow, dense structure of a saltmarsh provides a sheltered environment in which economically valuable species such as fish, shrimp, crabs, and oysters can proliferate and feed into offshore commercial fisheries benefitting their productivity and longevity (Whitfield 2017).

The role of saltmarshes in supporting biodiversity extends beyond economically valuable species that can be extracted by humans and extends to supporting biodiversity in adjacent environments as well. Saltmarshes support several resident and transient bird

populations that use the marsh as feeding, roosting, and nesting sites (Costa et al. 2001; Hughes 2004). For example, in the UK 60% of the common Redshank population nests in saltmarshes (Hughes 2004). Several passerines, waders, and geese also nest in saltmarshes (Hughes 2004). Birds can feed on invertebrates within the marsh or on adjacent mudflats, on seeds and the saltmarsh vegetation itself, and are provided with some protection from predation and disturbance by the saltmarsh (Costa et al. 2001; Hughes 2004). Saltmarshes also support biodiversity in adjacent habitats indirectly through services such as nutrient filtering. The uptake of nutrient-rich runoff from terrestrial habitats is an essential role that saltmarshes play in preventing the eutrophication of coastal waters (Barbier et al. 2011; Sousa et al. 2010). Without saltmarshes to filter terrestrial runoff, excess nutrients entering aquatic systems can promote algal blooms and the proliferation of resulting 'dead zones' due to hypoxic conditions in the water (Gedan et al. 2009).

Nutrient cycling is one of several regulating services saltmarshes provide; saltmarshes also regulate their environment through carbon sequestration, and shoreline protection from erosion and flooding (Adams et al. 2021). Saltmarshes are highly productive ecosystems which can rapidly sequester carbon thereby contributing to global climate regulation through the uptake of CO<sub>2</sub> (Beaumont et al. 2014; Chmura et al. 2003). Also, lower rates of decomposition due to anoxic conditions in saltmarsh soils prevents the quick turnover of carbon and allows for its long-term storage in the form of peat (Barbier et al. 2011). Saltmarshes as 'blue carbon' ecosystems could be an essential component of climate change adaptation strategies on national scales (Adams et al. 2021). Saltmarshes can further aid in adapting to the impacts of climate change by stabilising the coast against erosion (Spalding et al. 2014). The aboveground biomass of saltmarsh vegetation can resist and slow the flow of water over the canopy, encourage sediment to settle on the marsh, and trap it (Friedrichs & Perry 2001; Neumeier & Amos, 2006; Townend et al. 2011). The root network of the vegetation encourages the consolidation of this sediment on the platform (Chen et al. 2019; De Battisti et al. 2019). These mechanisms can slow rates of erosion (De Battisti et al. 2019; Spalding et al. 2014) and even cause vertical or lateral expansion of the marsh platform (Kirwan et al. 2016). The attenuation of wave energy over saltmarsh canopies due to resistance from the vegetation also directly protects coastal communities from flooding and storm surges (Möller et al. 1999, 2001; Leonardi et al. 2018). As natural defences against flooding and erosion, the presence of saltmarshes can reduce the vulnerability of coastal populations, infrastructure, and livelihoods to coastal hazards (Spalding et al. 2014; Temmerman et al. 2013). Wave energy attenuation by saltmarshes is especially relevant to this study and will be discussed further in section 2.3.

### 2.1.3. Anthropogenic impacts

Earth's coasts account for only about 4-5% of total land area but are home to over a third of its human population (McGranahan et al. 2007; UNEP 2006). This high density of human



settlement is associated with the many ecosystem services that coastal ecosystems provide in terms of the provision of natural resources and food, recreational and aesthetic value, protection from natural hazards and more (Costanza et al. 2008; Barbier et al. 2011; UNEP 2006). As such, coastal ecosystems have a long history of anthropogenic pressure from land reclamation for agriculture and infrastructure, invasive species and climate migrants, and eutrophication (Duarte et al. 2008; Gilby et al. 2021; Moser et al. 2012). Coastal wetlands are also vulnerable to the impacts of anthropogenic climate change and associated sea level rise and extreme weather (Duarte et al. 2008; Gilby et al. 2021; Moser et al. 2012).

Due to limited availability of data mapping the global extents of saltmarshes (Mcowen et al. 2017), it is difficult to exactly quantify their changes in extent over time. However, there are several studies and reports that indicate that saltmarshes have lost between 25% - 50% of their global historical coverage and have continued to decline at a minimum rate of 1–2% year<sup>-1</sup> (Duarte et al. 2008; Crooks et al. 2011; Gedan et al. 2009). A recent effort at mapping global wetland changes in extent by Murray et al. (2022) found that 1064 km<sup>2</sup> of saltmarsh coverage had been lost over 20 years from 1999 but that this was largely offset on a global scale by saltmarsh expansion. Of these changing wetlands extents, it was found that 27% were directly associated with anthropogenic activity (Murray et al. 2022). A leading direct anthropogenic cause of saltmarsh loss is land reclamation (Gedan et al. 2009). The practice of diking and draining saltmarsh land for agricultural conversion and salt production started in Europe as far back as the 11<sup>th</sup> century (Gedan et al. 2009; Knottnerus 2005). This practice of land conversion has continued though recently it has mainly been for the development of urban infrastructure (Gedan et al. 2009).

The proliferation of impervious surfaces at the coast due to urban development also leaves saltmarshes vulnerable to coastal squeeze (Torio & Chmura 2013). Accelerating sea level rise (SLR) poses an existential threat to saltmarshes due to submergence and erosion of marshland (Crosby et al. 2016; Kirwan et al. 2010). Saltmarshes can account for area loss at the seaward edge by expanding laterally inland (Kirwan et al. 2016) however, where this migration is obstructed by impervious surfaces (e.g. roads, buildings, flood protection barriers), the marsh is in danger of being 'squeezed' out of existence (Torio & Chmura 2013). Saltmarshes have displayed some resilience to this threat with accelerated rates of vertical accretion in response to accelerated SLR up to a threshold (Kirwan et al. 2010), even behind dykes where some saltmarshes have kept up with rates of SLR (Kirwan et al. 2016). However, decreased sediment supply to coastal marshes, due to human activities such as damming of rivers, reduce sediment available to support vertical accretion (Weston 2014).

Climate change also has the potential to modify saltmarshes beyond the direct threat of area loss. Increased frequency and intensity of storms have the potential to quickly input large volumes of sediment into the saltmarsh system and encourage marsh accretion (Giuliani & Bellucci 2019; Schuerch et al. 2013). Increasing storm frequency especially has been found to improve chances of saltmarsh survival under SLR conditions (Schuerch et

al. 2013). Meanwhile, the increasing intensity of storms has the potential to deliver larger amounts of sediment to a saltmarsh in a single event (Schuerch et al. 2013), but much of this massive sediment influx may not be retained by the saltmarsh vegetation (Boorman 1999) and therefore not result in elevation of the marsh surface. Also, more intense storms can cause damage to the marsh itself through erosion at the seaward edge (Crosby et al. 2016) though saltmarshes are generally able withstand this impact without collapsing (Leonardi et al. 2018). Long-term effects of increasing storminess and erosion at saltmarsh sites can include the gradual deepening of tidal flats, encouraging higher wave energy propagation even during normal conditions which can adversely impact saltmarshes (Leonardi et al. 2018). The impacts of increasing extreme weather events on saltmarshes is highly variable and dependant on multiple factors (Leonardi et al. 2018) which highlights the importance of site-specific monitoring.

Furthermore, changes in environmental conditions due to climate change and direct human impacts have had significant effects on the species, biodiversity, and complexity of saltmarshes. Following the global trend of shrubification – the expansion of shrubs poleward in response to the impacts of climate change - mangrove forests are migrating poleward due to rapid warming and sea level rise and encroaching on previously saltmarsh-dominated land (Rogers et al. 2006; Saintilan et al. 2014). This is thought to be happening due to increased inundation frequencies at declining marsh elevations and increasing temperatures; conditions that favour mangroves over saltmarsh vegetation (Rogers et al. 2006). Species composition has also been altered historically by humans introducing non-native species to saltmarshes (Gedan et al. 2009; Lotze et al. 2006; Newton et al. 2020). In many cases, non-native species have been introduced to coastal environments by humans for their productivity and role in coastal defence, but their proliferation often outcompetes native species causing structural changes to the marsh environment (Gedan et al. 2009). In some cases, though the introduction of non-native saltmarsh vegetation has caused a decrease in the extent of native saltmarsh plants, the success of the invasive species can result in an overall increase in saltmarsh area (Gu et al. 2018). On the other hand, invasive species can outcompete native species to form homogenous stands thereby decreasing the floral biodiversity and complexity of the marsh (Zedler & Kercher 2004). The proliferation of invasive species also changes the habitat structure of the saltmarsh to the extent that the habitat is no longer suitable for native invertebrates; this has been observed to decrease native invertebrate abundance and diversity (Brusati & Grosholz 2006).

Pollution and eutrophication due to human activities can also destabilise saltmarsh environments (Deegan et al. 2012; Gedan et al. 2009; Newton et al. 2020), which can, in turn, make them more vulnerable to further disturbances such as the invasion of non-native species (Zedler & Kercher 2004). Nitrogen-rich urban and agricultural runoff entering saltmarsh environments can overwhelm their capacity for nutrient uptake (Giuliani & Bellucci 2019) and cause conditions under which invasive species can

outcompete and displace native saltmarsh vegetation (Zedler & Kercher 2004). The competitive balance of saltmarshes is also altered by nutrient pollution where plant competition in nutrient-low soils result in high species richness and zonation; all of which can be lost due to eutrophication (Bertness et al. 2002). Eutrophication has also been associated with decreased stability of the marsh platform due to the combined effects of decreased below-ground root biomass accumulation and increased decomposition rates (Deegan et al. 2012). Roots retain and consolidate sediments on the marsh platform, strengthening the platform against erosion, gravitational slumping, and cracking (De Battisti et al. 2019; Deegan et al. 2012). Nutrient enrichment alters biomass allocation in saltmarsh species, encouraging the growth of above-ground leaf biomass at the expense of below-ground roots (Deegan et al. 2012). As the bank weakens and cracks due to reduced root biomass, a positive feedback loop can form wherein marsh platform destabilisation allows further intrusion of nutrient-enriched water into the sediment encouraging higher rates of decomposition of peat which further destabilises the marsh platform leaving it vulnerable to erosion and collapse (Deegan et al. 2012).

The health, stability, and composition of a saltmarsh are all key factors in their survival and the continued delivery of valuable ecosystem services. All these factors rely on a complex network of biogeomorphodynamic interactions which are undergoing rapid changes due to anthropogenic pressures directly and indirectly. It is therefore increasingly imperative to develop accessible tools that can monitor conditions in saltmarshes on fine scales spatially and temporally to gain a better understanding of how they are being impacted.

## 2.2. Coastal defence

Coastal floods are caused by extreme storm surges and often entail severe winds and waves and a temporary rise in sea level, sometimes by several meters (Resio & Westerink 2008). These events are projected to become more frequent and more extreme in the coming years under climate change conditions due to increasing storminess, sea level rise, and land subsidence (Kaya et al. 2005; Rennie & Hansom 2011; Wong et al. 2014). The damage these events cause to coastal populations and infrastructure can be severe (Kaya et al. 2005) and as populations in coastal settlements continue to grow rapidly a growing number of people are vulnerable to this hazard. This issue has traditionally been answered with engineering solutions such as the building of sea walls, groins, embankments, and dykes. Under climate change conditions however, these traditional engineering solutions are proving unsustainable due to the cost of maintaining and updating them (Temmerman et al. 2013). Therefore, as the limitations of traditional engineering solutions become evident, there is increasing interest in the conservation, creation, and restoration of coastal habitats such as saltmarshes as a nature-based approach to coastal protection (Pétillon et al. 2023; Spalding et al. 2014; Stark et al. 2016; Sutton-Grier et al. 2015; Temmerman et al. 2013). Saltmarshes support several co-benefits as well as providing a cost-effective and self-adaptive alternative to traditional

engineering approaches to coastal defence (Barbier et al. 2011; Silinski et al. 2018).

Saltmarshes can attenuate waves and  $C_v$  thereby protecting coastal areas from flooding and erosion (Section 2.3). The complexity of vegetation-hydrodynamic interactions that creates this attenuation effect is now starting to be captured in field and modelling studies (Garzon et al. 2019; Möller et al. 1999; Rupprecht et al. 2017; Yang et al. 2012). Though hydrodynamic energy attenuation varies spatially and temporally depending on multiple factors (Fagherazzi et al. 2020; Leonardi et al. 2018), there is evidence of their value as coastal defence structures (Möller & Spencer 2002; Möller 2006). For example, significant reductions in storm surge levels and hurricane damage have been observed as a direct result of hydrodynamic energy attenuation over saltmarshes (Costanza et al. 2008). This is a valuable service by itself; however, conventional engineering design is also generally highly effective at reducing risk to specific standards taking several environmental factors into consideration (Stark et al. 2016; Temmerman et al. 2013).

The main advantages that saltmarshes offer as coastal defence structures over traditional designs are their capacity to adapt to changing physical conditions over longer timescales (Fagherazzi et al. 2020; Silinski et al. 2018). For example, saltmarshes can capture and trap sediments leading to a vertical accretion of the saltmarsh platform that, at some sites, has kept pace with sea level rise (Kirwan et al. 2010, 2016; Schuerch et al. 2013). In the case of traditional structures, keeping them updated according to predictions often includes heightening them, lengthening them or other construction that is costly and not always sustainable in a time of rapid change (Spalding et al. 2014). A saltmarsh can migrate laterally to preserve itself (Fagherazzi et al. 2020) though this ability can sometimes be restricted in highly developed areas (Torio & Chmura 2013). This is in contrast to traditional structures which are hard and fixed.

Saltmarshes also have the capacity to self-repair in response to constant hydrodynamic action and regenerate after damage from extreme weather (Leonardi et al. 2018). Saltmarsh communities are made up of deciduous perennial plant species that follow a seasonal cycle of vegetation green-up and die-off allowing them to replenish their biomass annually. Also, in comparison to other ecosystems, saltmarshes are relatively resistant to storm damage (Fagherazzi 2014; Leonardi et al. 2018). In the case of some more flexible saltmarsh species, their flattening during storm conditions protects the marsh surface from erosion (Leonardi et al. 2018). It has even been suggested that storm surges can be beneficial to saltmarshes by causing a large influx of sediment into their environment (PannoZZo et al. 2021). Saltmarsh vegetation can trap and consolidate this sediment to facilitate vertical accretion thereby elevating the marsh platform which enables them to better resist future storms (Smolders et al. 2015; Stark et al. 2016). Traditional coastal defence structures cannot dynamically respond to their environment in this way. These hard, man-made structures are subject to wear over time and damage during storm events so, as storminess increases due to climate change, more frequent, intensive maintenance is likely to be needed adding to the growing cost of hard coastal

engineering (Spalding et al. 2014).

Traditional engineering solutions have no capacity for self-repair or regeneration and furthermore can hinder the capacity of surrounding wetlands to do so (Spalding et al. 2014). The installation of hard structures on the coast can change sediment input and dynamics and alter tidal flows in such a way that causes land subsidence and the subsequent loss of saltmarsh extents in the area (Da Lio et al. 2018; Syvitski et al. 2009). Also, the landward migration of saltmarshes in response to rising sea levels can be restricted by the presence of these impervious structures which accelerates the loss of saltmarshes to coastal squeeze (Torio & Chmura 2013). In contrast, the presence of healthy saltmarsh communities on the coast can provide benefits beyond coastal protection (Spalding et al. 2014). Co-benefits that saltmarshes provide include the provision of food and building materials to coastal communities, supporting marine biodiversity and thereby increasing the productivity of nearby fisheries, carbon sequestration, and recreational opportunities (Barbier et al. 2011). Meanwhile traditional engineered structures are monofunctional.

However, traditional engineering structures do have the advantage of providing high levels of risk reduction relative to a smaller footprint (Spalding et al. 2014). The attenuation capacity of a saltmarsh has been found to increase with an increase in the width and continuity of the vegetated community (Leonardi et al. 2018) thereby requiring a larger spatial footprint for adequate coastal protection. In general, traditional engineering solutions for coastal protection can provide more reliable, predictable results. The coastal protection capacity of natural systems such as saltmarshes can vary spatially and temporally and the factors that influence this variation have started to be studied more rigorously in the past decade (Leonardi et al. 2018; Pétillon et al. 2023). These studies are contributing towards understanding how to assess the hydrodynamic energy attenuation capacity of marshes which is information without which ecosystems cannot be relied upon to provide adequate coastal defence (Pétillon et al. 2023). In some cases, this can necessitate greater safeguards behind saltmarshes due to the uncertainty of their effectiveness (Spalding et al. 2014). In the meantime, traditional engineered structures have been designed specifically for, and been successful at, protecting coasts.

Overall, there are many advantages to implementing nature-based solutions for coastal defence. However, due to the current gaps in our knowledge about the physical thresholds that impact ecosystem service delivery, these solutions are not always reliable (Spalding et al. 2014). Reliably reducing risk is an essential element of effective coastal protection that is provided more effectively by traditional engineering solutions (Temmerman et al. 2013). A hybrid solution may be optimal for coastal protection under these circumstances (Stark et al. 2016; Sutton-Grier et al. 2015). Utilising ecosystems alongside conventional coastal defence structures has the benefit of the risk reduction certainty of the traditional engineering approach, and the co-benefits from the nature-based approach. Ecosystems used as coastal defence in front of hard structures such as sea walls has even been observed to protect these structures from hydrodynamic energy

thereby reducing the costs of maintenance and updating (Möller & Spencer 2002). For example, managed realignment, whereby maintained defences are set back and intertidal habitats are encouraged to reclaim the land between the old and new line of defences, is a hybrid strategy that has grown in use in Europe and North America in recent decades (Rupp-Armstrong & Nicholls 2007). This kind of active consideration of ecosystems in coastal management and planning is a step towards more sustainable solutions for coastal defence.

## 2.3. Hydrodynamic energy attenuation in saltmarshes

### 2.3.1. Benign conditions

Saltmarshes can protect coastal areas from flooding and erosion by attenuating hydrodynamic energy (Möller et al. 1999; Leonardi et al. 2018; Yang et al. 2008). Landward dampening of hydrodynamic energy is generally observed in coastal environments due to increasing elevation (Möller et al. 1999, 2001). For example, studies have found that unvegetated sandflats and mudflats alone can attenuate wave energy by up to 29% and reduce wave heights by up to 15% (Möller et al. 1999, 2001). However, the significantly increased rates of wave and current attenuation observed over saltmarsh vegetation canopies in field studies (Garzon et al. 2019; Möller et al. 2001; Yang et al. 2008) cannot be accounted for by hydrodynamic conditions alone (Möller et al. 1999). Vegetated communities have been found to attenuate waves (Möller et al. 1999, 2001; Möller & Spencer 2002; Ysebaert et al. 2011) and current velocities ( $C_v$ ) (Yang et al. 2008; Bouma et al. 2005a), and reduce storm surge heights (Leonardi et al. 2018; Wamsley et al. 2009), by resisting hydrodynamic flow. These dampening effects are induced by increased surface roughness and friction over the canopy, hydrodynamic drag within the vegetation, and depth-induced wave dampening and shoaling (Möller et al. 1999; Möller & Spencer 2002). The attenuating effect of saltmarsh vegetation has been well established in both field (Cooper 2005; Garzon et al. 2019; Möller et al. 2001; Yang et al. 2008) and flume (Möller et al. 2014; Rupprecht et al. 2017) studies, however, there are large variations in the observed rates of attenuation between studies (Table 1). The contents of Table 1 exemplifies how the data ranges between studies in terms of average attenuation rates of hydrodynamic energy (wave height, wave energy, and  $C_v$ ) over saltmarsh vegetation under benign weather conditions. This spatial and temporal variation of attenuation rates occurs due to several factors including the topography of the marsh, hydrodynamic conditions, biophysical properties of the vegetated community, seasonality and weather conditions (Möller & Spencer 2002; Leonardi et al. 2018; Schulze et al. 2019).

Table 1. Magnitudes of hydrodynamic energy attenuation by different saltmarsh species reported in published studies.

Paper	Hydrodynamic Parameter	Reduction of Hydrodynamic Parameter (%)	Saltmarsh Transect Length	Notes
Cooper 2005	Wave height	94%	425m	<i>Puccinellia maritima</i> and <i>Salicornia europaea</i>
	Wave energy	99%		
	Wave height	69%	542m	<i>Atriplex portulacoides</i> and <i>Spartina alterniflora</i>
	Wave energy	79%		
	Wave height	85%	387m	<i>Atriplex portulacoides</i> and <i>Salicornia europaea</i>
	Wave energy	96%		
Möller et al. 1999	Wave energy	82%	180m	Field measurements, Stiffkey marshes
Möller et al. 2001	Wave height	61%	180m	Field measurements, Stiffkey marshes
Möller & Spencer 2002	Wave height	87.37%	163m	Tillingham saltmarsh, gentle slope
	Wave energy	98.92		
	Wave height	43.81%	10m	Bridgewick saltmarsh, cliff
	Wave energy	79.13%		
Yang et al. 2008	Wave height	16%	16.5m	<i>Scirpus mariqueter</i>
	Wave height	37%	13.5m	<i>Spartina alterniflora</i>
	$C_v$	0.97%/m (~87.3%)	90m	Mixed marsh, Chongming
Ysebaert et al. 2011	Wave height	Up to 80%	<50m	<i>Scirpus mariqueter</i> <i>Spartina alterniflora</i>

Differences in the bed topography of saltmarshes can have significant impacts on rates of hydrodynamic energy attenuation (Möller & Spencer 2002). A study by Möller & Spencer (2002) compared attenuation rates at two saltmarsh sites with differing topographies at their seaward edges at the Dengie marshes, England. Though part of the same marsh system, significant differences in attenuation of wave heights and energy could be observed between the two sites. The cliff site was less effective at attenuating waves overall compared to the site with sloped seaward topography (Table 1) and wave shoaling at the cliff edge was observed to increase wave height (Möller & Spencer 2002). However, shoaling leads to the wave breaking which should contribute to a reduction of wave energy (Mendez & Losada 2004) which may have contributed to the ultimately positive attenuation values at the cliff site (Table 1) despite the initial wave height increase.

Hydrodynamic conditions at saltmarsh sites are also a driver of spatial and temporal

variability in hydrodynamic energy attenuation (Cooper 2005; Leonardi et al. 2018; Möller 2006). Over any coastal surface, hydrodynamic conditions significantly impact the rate of landward hydrodynamic energy attenuation (Augustin et al. 2009; Le Hir et al. 2000; Möller 2006). For example, greater tidal amplitudes are accompanied by increased  $C_v$  at greater heights above the unvegetated sediment surface (Bouma et al. 2005a). This relationship holds true within saltmarsh vegetation as well though  $C_v$  were observed to be a magnitude lower within the saltmarsh canopy (Bouma et al. 2005a). Furthermore, water depth and incident wave height are a significant control factor for the attenuation of waves over unvegetated coastal surfaces (Le Hir et al. 2000). These conditions can also significantly impact wave attenuation within saltmarshes (Möller et al. 2001; Möller & Spencer 2002). In the case of the Stiffkey marshes in England, the negative relationship between water depth and wave attenuation was found to be more apparent over saltmarsh than over unvegetated surfaces (Möller et al. 2001). On the other hand, just down the coast at the Dengie marshes, water depth was observed to have little relevance to wave attenuation rates outside of the seaward edge of the vegetation (Möller & Spencer 2002). Though the extent of the impact of hydrodynamics is evidently very site-specific, in both cases hydrodynamic conditions have some effect on the attenuating capacity of the saltmarsh.

The vegetation-hydrodynamic interactions and attenuation capacity of a saltmarsh are most directly impacted by the structure and biophysical properties of the vegetation itself (Schulze et al. 2019). Though water depth is a significant hydrodynamic parameter for determining attenuation, within a saltmarsh canopy it is important to consider water depth in relation to plant height (Garzon et al. 2019). A laboratory experiment by Augustin et al. (2009) concluded that emergent plant stems attenuated hydrodynamic energy more effectively than fully submerged stems. This was observed in the field by (Yang et al. 2012) where overall taller vegetated communities dissipated hydrodynamic energy more efficiently and stem submergence – the ratio of water depth to plant height – was found to be inversely correlated to plant height. Stem flexibility can also influence hydrodynamic energy attenuation capacity where increasing plant flexibility causes less flow resistance and therefore less efficient attenuation (Bouma et al. 2005b). These vegetation characteristics will be specific to the growing conditions and species compositions at different saltmarsh sites.

The efficiency with which vegetation can resist hydrodynamic flow varies between species (Bouma et al. 2005b; Schulze et al. 2019). For example, Yang et al. (2008) observed that the taller, densely growing *Spartina alterniflora* was more effective at attenuating wave heights compared to *Scirpus mariqueter* which has relatively lower above-ground biomass as it is, on average, shorter and grows less densely. There are several studies that have made similar observations of significant differences in attenuation capacities between plant species due to their characteristic biophysical properties (Rupprecht et al. 2017). Furthermore, there is evidence to suggest that growing conditions such as salinity levels, lengths of inundation, and differences in exposure to



hydrodynamic energy can cause species to prioritise characteristics such as height and diameter differently thereby possibly altering these biophysical properties both within and between saltmarsh sites (Schulze et al. 2019). This will cause spatial variation of the attenuation capacity of saltmarshes according to species composition and growing conditions.

Temporal variation of the attenuation capacity of saltmarsh vegetation has also been observed due to changes in plant biophysical properties across seasons (Möller & Spencer 2002; Schulze et al. 2019). A study by Schulze et al. (2019) found that in two common saltmarsh plants, both plant stem flexibility and aboveground biomass varied significantly from Spring to Summer. Similarly, a study by Möller & Spencer (2002) found that vegetation density varied significantly between seasons and generally peaked in November at their study site. This study also found that wave energy attenuation varied seasonally and that it was greatest from September to November and lowest in spring from March to July which was positively associated with seasonal vegetation growth at this site (Möller & Spencer 2002).

It is evident that the attenuation capacity of saltmarshes is greatly influenced by several key factors including marsh topography, hydrodynamic conditions, and plant biophysical properties. These factors can vary greatly between different saltmarsh habitats contributing to the site-specificity of attenuation capacity. Tools that facilitate long-term, detailed measurements of hydrodynamics within saltmarsh canopies would therefore be valuable for obtaining field measurements that provide insights into hydrodynamics within saltmarsh canopies at multiple spatial and temporal scales. This would be useful for gaining a deeper understanding of saltmarsh attenuation potential at specific sites and for identifying patterns across different saltmarsh habitats.

### 2.3.2. Storm conditions

Weather conditions can also cause variations in vegetation-hydrodynamic interactions. Hydrodynamics within saltmarsh vegetation have mostly been monitored under benign conditions (Rupprecht et al. 2017). The attenuation capacity of saltmarshes during storm events predicted in the literature is therefore usually based on flume experiments (Möller et al. 2014), proxy values such as damage reduction in coastal settlements (Costanza et al. 2008), and hydrodynamic modelling (Sheng et al. 2012). A flume experiment by Möller et al. (2014) found that saltmarsh vegetation could dissipate waves of up to 1m by up to 20% at 40m from the seaward edge even at the increased water depths expected during storm conditions. Field measurements by Garzon et al. (2019) during storm conditions found that higher waves of up to 1.55m were dissipated by up to 50% at 250m from the saltmarsh edge. Peaks of storm surge levels have also been found to decrease significantly behind saltmarshes (Wamsley et al. 2009). On average, peak surge levels have been reduced by 1m for every 14.5km that the surge has flowed over saltmarsh vegetation during hurricane events (Wamsley et al. 2010). However, similarly to benign conditions, hydrodynamic energy attenuation during storms is complex and varies greatly

depending on storm characteristics and saltmarsh habitat and ecosystem properties (Leonardi et al. 2018).

The efficacy with which a vegetated saltmarsh community can attenuate hydrodynamic energy under storm conditions relies on marsh width, topography, and species composition (Leonardi et al. 2018; Stark et al. 2016). Storm surge and hydrodynamic energy attenuation is species specific according to plant biophysical properties. For example, in a study comparing two common saltmarsh species - *Elymus athericus* and *Puccinellia maritima* - it was found that the taller, stiffer *E. athericus* was more effective than the low-growing *P. maritima* at attenuating waves at lower water levels (Rupprecht et al. 2017). With long wave periods and higher water levels as might be expected in a storm, however, *P. maritima* was observed to dissipate waves by up to 35% while *E. athericus* did not cause any significant attenuation under these conditions (Rupprecht et al. 2017). In general, it is thought that more flexible vegetation conforms more to the dominant direction of hydrodynamic flow at a high angle providing less resistance and therefore lower rates of attenuation (Bouma et al. 2005b) however this example evidences the complexity of vegetation-hydrodynamic interactions.

Furthermore, wider saltmarshes, on more elevated platforms, with a more continuous canopy are generally expected to attenuate hydrodynamic energy more effectively (Leonardi et al. 2018; Sheng et al. 2012; Stark et al. 2016). This suggests that saltmarsh degradation from erosion and sediment depletion could negatively impact the attenuation capacity of saltmarshes (Temmerman et al. 2012). Also, a modelling study by Sheng et al. (2012) found that attenuation in saltmarsh vegetation increased with increased storm intensity and greater forward speed due to onshore winds lasting for a relatively shorter period. Longer storms and slower storms are associated with a relative reduction in attenuation by saltmarsh vegetation (Sheng et al. 2012; Wamsley et al. 2010). These less violent storms are also associated with relatively greater morphological damage to the saltmarsh (Leonardi et al. 2018). Vegetation can be lost and damaged due to flattening during storm events; more flexible vegetation has been found to be more resistant to storm damage while stiffer stems are more prone to breakage (Möller et al. 2014; Rupprecht et al. 2017). Also, though stiffer plant species can more effectively resist hydrodynamic flow and contribute to storm surge reduction, they can increase turbulence and scour while the flattening of more flexible plants can shield the marsh surface from erosion (Leonardi et al. 2018).

### 2.3.3. Impact of plant traits on attenuation capacity

Biophysical characteristics of saltmarsh plants and vegetation communities have an impact on their capacity to attenuate hydrodynamic energy. For example, plant stem density is known to profoundly impact attenuation capacity where higher plant density more efficiently diffuses waves (Leonard & Croft 2006; Leonard & Luther 1995; Neumeier & Ciavola 2004). Plant density ( $d$ ) can be measured as the number of stems per  $m^2$ . Another factor that can significantly influence the rate and magnitude of hydrodynamic

energy attenuation is the seaward-facing surface area of the vegetation (Figuroa-Alfaro et al. 2022; Mendez & Losada 2004). This can be expressed as a single parameter – the Frontal Surface Area (FSA) - derived from plant height ( $h$ ), plant basal diameter ( $Bd$ ), and the number of plants per unit area (density,  $N$ ):  $FSA = h \times d \times Bd$  (Figuroa-Alfaro et al. 2022). As FSA increases, rates of attenuation are expected to increase (Figuroa-Alfaro et al. 2022). Finally, the attenuation capacity of saltmarsh species will also be impacted by the mechanical stability of the plant (Bouma et al. 2005b). The slenderness coefficient ( $S$ ), defined as the ratio of height ( $h$ ) to basal diameter ( $Bd$ ), ( $S = h / Bd$ ) is an indicator of mechanical stability where greater slenderness indicates lower mechanical stability (Chatagnier 2012; Vovides et al. 2014). Therefore, as slenderness increases and a plant's ability to withstand mechanical stress decreases, attenuation capacity is expected to decrease.

The body of research on these biophysical mechanisms of hydrodynamic energy attenuation in saltmarshes has grown in the past decade but is usually explored through the lens of how plants impact their physical environment (Pétillon et al. 2023). However, there is evidence that environmental conditions can impact plant morphology and physiology (Shao et al. 2020; Silinski et al. 2018). For example, Shao et al. (2020) found that increased wave exposure suppresses stem height in *Spartina alterniflora* and increases belowground biomass allocation. This will have implications for ecosystem service delivery and the capacity of saltmarsh vegetation to attenuate hydrodynamic energy. The impact that abiotic conditions have on saltmarsh plants will inform the long-term efficacy of nature-based solutions for flooding, but it is an area that is currently understudied (Pétillon et al. 2023).

## 2.4. Monitoring Coastal Hydrodynamics

Hydrodynamics are an important driving force behind wetland system dynamics across a range of ecosystems both spatially and temporally (Allen 2000). Tidal characteristics at a saltmarsh determine their elevational limits (Balke et al. 2016), impact seedling establishment (Balke et al. 2014) and impact the stability of the marsh in response to sea level rise (Kirwan & Guntenspergen 2010). Shifts in tidal channels impact the exposure of saltmarshes to wave and currents (Ladd et al. 2021) and exposure to wave and currents influences erosion and expansion of the marsh (van der Wal & Pye 2004). Hydrodynamic monitoring has proven to be an essential prerequisite for designing coastal restoration programs and monitoring their success (Balke et al. 2021; Billah et al. 2022). Long-term, detailed records of coastal hydrodynamics are therefore essential to better understand, protect, and restore coastal ecosystems (Waltham et al. 2020) and to better understand and assess their ecosystem services (Möller et al. 2014).

There are a variety of commercially available sensors that reliability monitor fine-scale and have been traditionally used for these monitoring purposes. However, traditional hydrodynamic monitoring equipment often has the drawback of depending on existing

infrastructure or being high-cost and requiring specialist knowledge to operate. Records from nearby tide gauges or in-situ pressure sensors can be used to derive inundation frequency and duration at a site (Balke et al. 2021) but this relies on a pre-existing tide gauge close to the study site for reliable data. Pressure sensors can be calibrated to collect pressure data from which inundation depth, duration, and frequency can be derived. Equipment such as acoustic Doppler velocimeters (ADV), acoustic Doppler current profilers (ADCPs), and electromagnetic flow meters (EMFs), can be used to measure  $C_v$  and direction (for example, (Möller et al. 2014)). Though they are reliable, these tools are expensive and are therefore usually only deployed for short periods during specific studies to avoid theft or damage. Monitoring infrastructure is also expensive to maintain and not always available for every study site. All these factors hinder the accessibility of consistent, continuous, high resolution hydrodynamic data in coastal habitats.

As an alternative to these sensors, inertial measurement unit sensor technology is being rapidly developed and increasingly being deployed to monitor natural systems (Balke et al. 2021; Maniatis, 2021). Inertial measurement unit sensors are mobile, usually more cost-effective, sensors which include micro electrical mechanical systems such as accelerometers, gyroscopes, and magnetometers (Maniatis, 2021). Over the last 15 years, the use of this technology has become well established in fields such as geomorphology (Maniatis, 2021) and is now starting to be applied more frequently to hydrodynamic research (Balke et al. 2021). Dip-current meters, which incorporate accelerometers, have been used to measure the velocity of waves and currents in coastal waters (Figurski et al. 2011; Hansen et al. 2017). The Mini Buoy incorporates accelerometers to monitor current velocities, wave orbital velocities, and inundation duration and frequency in intertidal settings (Balke et al. 2021). The use and development of this technology is still very much in its infancy, and it is important to note that its use in monitoring natural systems still requires exploration and refinement (Maniatis, 2021).

#### 2.4.1. The Mini Buoy

The Mini Buoy is a customisable, drag-tilt current sensor and a more accessible alternative to traditional hydrodynamic monitoring methods (Balke et al. 2021). Components of the Mini Buoy (Figure 1) are commercially available and inexpensive compared to traditional, specialist equipment. The Mini Buoy is also associated with a custom-built Mini Buoy App that allows users to input data for analysis, interpretation and recommendations (Balke et al. 2021; Ladd et al. 2024a). Also, Mini Buoys are small and easy to transport, have been updated to be more durable in tidal environments (Ladd et al. 2024a), and a detailed guide is available on how to assemble them (Ladd et al. 2024b).



Figure 1. Mini Buoys tethered to the ground. A) B4+ model of the Mini Buoy B) Pendant model of the Mini Buoy

The Mini Buoy contains an acceleration data logger which records acceleration along the x-y-z axes as G-forces (where  $1G = 9.81 \text{ m s}^{-2}$ ) from which tidal inundation characteristics (duration and frequency) and  $C_v$  can be derived; more recent models can also measure wave orbital velocities (Balke et al. 2021; Ladd et al. 2024a). To develop this tool, the Mini Buoy was deployed mudflats in a former aquaculture pond area in Indonesia, and in the Bay of Fundy in Canada where its outputs were calibrated against industry-standard water level and  $C_v$  sensors (Balke et al. 2021). It has since been used to support a variety of studies monitoring coastal hydrodynamics to support research on mangrove biodiversity and restoration (Basyuni et al. 2022; Hasibuan et al. 2021) and the biomechanical properties of saltmarsh vegetation (Keimer et al. 2023). However, in each case Mini Buoys have been deployed only on tidal mudflats on the fringes of coastal vegetation with no studies thus far investigating how they perform within the canopy. Widening the application of the Mini Buoy to monitor hydrodynamics within coastal vegetation would provide a wealth of information on vegetation-hydrodynamic interactions for researchers and coastal planners.

Although there are many advantages to the Mini Buoy, there are several limiting factors to consider when using them; their durability, sensitivity to low  $C_v$ , memory/battery capacity, and the effort it takes to assemble them. There are now three models of the Mini Bouy available which each offer their own advantages. The original Mini Buoy, the B4, was found to degrade over time, has a detection limit of  $0.043 \text{ ms}^{-1}$ , and cannot measure wave orbital velocities (Ladd et al. 2024a). The updated B4+ model was presented in an effort to improve on all of these limitations. Designed to be more durable, the B4+ has its acceleration logger housed within a UV-protected centrifuge tube and is thoroughly waterproofed with a rubber O-ring around the inside of the lid (

Figure 2) and the outer lid sealed with silicone sealant (Ladd et al. 2024a). Also, the B4+ has been calibrated to measure wave orbital velocities at a minimum sampling rate of

10s, has a lower detection limit of  $0.018 \text{ ms}^{-1}$ , and has demonstrated increased sensitivity to waves and currents due to the addition of 20g of lead shot weight (Ladd et al. 2024a).

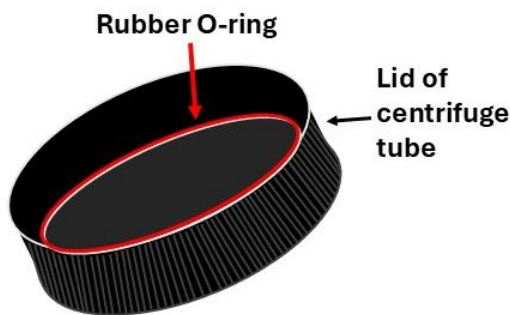


*Figure 2. Diagram of the placement of the rubber O-ring inside the lid of the centrifuge tube when assembling the B4+ Mini Buoy.*

The Pendant model, also presented in Ladd et al. (2024a), uses the Pendant HOB0 G accelerometer which is housed in a float as factory standard and is therefore less effort to assemble than the B4+. It can also measure wave orbital velocities at a minimum sampling rate of 10s and has a detection limit of  $0.049 \text{ ms}^{-1}$  (Ladd et al. 2024a). The duration of deployment for the Pendant is limited by its memory capacity of 64 KB which would only allow it to be deployed for  $\sim 8$  days when sampling at 10s. This length of deployment would not be fully representative of a full tidal cycle and as such it is recommended that surveys last at least 15 days (Ladd et al. 2024a). In contrast, even at a higher sampling rate of 1s, the B4+ can be deployed for  $\sim 25$  days. However, as Mini Buoys can only measure  $C_v$  when they are fully inundated, the total height of the model should also be considered when deployed in environments with shallow water depths. The B4+ is 155 mm in length while the Pendant is 108 mm. The smaller Pendant model will require less water depth to begin producing  $C_v$  outputs which may be better suited to measuring along transects that rise in elevation as is the case in this study. In any case, comparing the use of multiple models of the Mini Buoy in different research contexts to compare how they perform will enable us to make informed recommendations on which environments and research goals they are best suited for to facilitate their usage for coastal managers.

## 3. Methods

### 3.1. Field Site

The Clyde Estuary is the largest on Scotland's west coast and is situated inland of the Firth of Clyde. The estuary is long and narrow and extends 40km from Greenock to the City of Glasgow (Karunarathna 2011). Tides in the estuary are semi-diurnal and have spring and neap tidal ranges of 3.0m and 1.9m respectively (Karunarathna 2011). The mouth of the estuary is mostly sheltered from wave penetration from the Firth of Clyde, so wave heights are largely dependent on local wind conditions, and tidal currents are mostly weak with velocities below  $0.5 \text{ m s}^{-1}$  (Cressey & Johnson 2004; Firth & Collins 2002) creating an environment with overall low hydrodynamic energy. Tidal asymmetry has been observed

in the Clyde Estuary with greater ebb tide velocities compared to flood tide velocities (Brown et al. 2024). The main freshwater inputs into the estuary are from the River Clyde and its five tributaries (the Rivers Kelvin, White Cart, Black Cart, Gryffe and Leven) which altogether average an annual freshwater flow of  $110 \text{ m}^3\text{s}^{-1}$  and an estimated 50-year flood flow of  $1438 \text{ m}^3\text{s}^{-1}$  (Bekic et al. 2006). A pattern of increasing seasonal variability of flow volume into the Clyde estuary has been observed (Jones & Ahmed 2000).

The morphology of the Clyde Estuary has been heavily influenced by human settlement on its banks. The Clyde Estuary is inhabited by the city of Glasgow, Scotland's most densely populated city ( $3400 \text{ people/ km}^2$ ) (World Population Review 2024). Because of its association with the city of Glasgow, the environment of the Inner Clyde Estuary has a long history of pressures from urbanisation and heavy industry. The River Clyde has been continuously dredged over the last 200 years for shipping and navigation, structures such as embankments and seawalls have been implemented for flood protection, and built-up areas continue to replace the Clyde Estuary's inter-tidal environments as Glasgow's population continues to grow (World Population Review 2024). Despite this, the Inner Clyde Estuary continues to host a variety of morphological features including sandflats, mudflats, and some areas of saltmarsh. Extensive mudflats can be found throughout the Inner Clyde Estuary at sites including Dumbarton, the field site in this study. Several areas of saltmarsh have also been identified in the Inner Clyde Estuary including an extensive area in Dumbarton. The value of these wetland environments is recognised nationally and internationally by the Inner Clyde Estuary's designation as a Ramsar wetland, a European Commission (EC) Special Protection Area, and a Site of Special Scientific Interest. A total extent of 41 ha of saltmarshes inhabits the Inner Clyde Estuary (Haynes 2016). There are well-established but fragmented communities on both banks of the River Clyde. On the north bank these spread across several sites from Dumbarton Castle to Ardmore (Figure 3; Hansom et al. 2017) including a community at Dumbarton itself. On the south bank saltmarsh vegetation can be found along the Black and White Cart tributaries near Glasgow Airport, Newshot island, Longhough point and Langbank East Crannog (Figure 3).

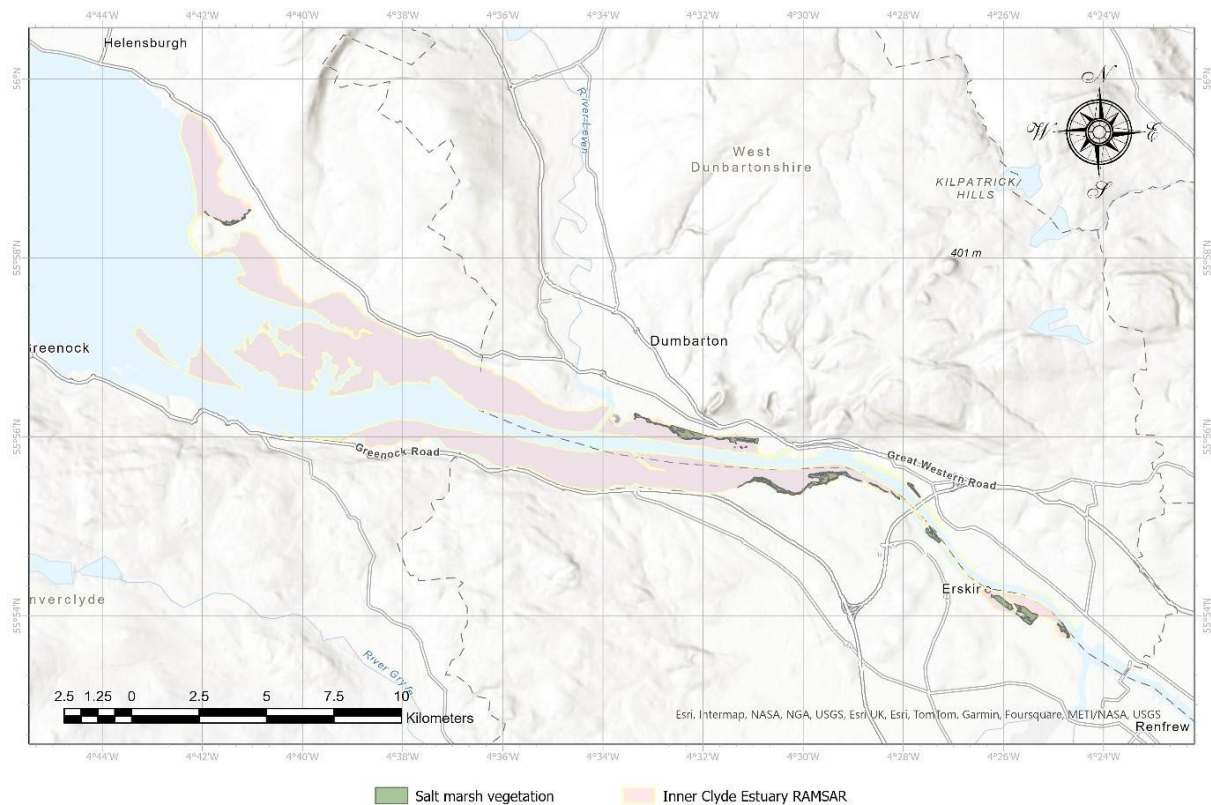


Figure 3. Salt marsh distribution (green polygons) along the Inner Clyde Estuary Ramsar site (pink polygon). Source: map adapted from NatureScot (Haynes 2016).

The field site at Dumbarton on the northern bank of the River Clyde was chosen for this study due to the large, distinct, monospecific stands of both *Bolboschoenus maritimus* and *Phragmites australis* that are found there. A significant proportion (43.9%) of the saltmarshes of the Inner Clyde Estuary are made up of these brackish species and by some accounts their extent in Scotland is growing (Haynes 2016). As an increasingly prominent feature of Scotland’s shoreline, it is important to the implementation of nature-based solutions to flooding that the Cv attenuation capacities of these brackish species be better understood. Therefore *B. maritimus* and *P. australis* were chosen as the focal species of this study. At Dumbarton both species grow in distinct, reasonably monospecific belts that spread more than 10m inland allowing for uniform transects to be set up within them for hydrodynamic monitoring. Transects were set up perpendicular to the main channel of the River Clyde starting on the mudflat and ending 10 m into the vegetation. A total of six 10 m transects (3 transects per species) were delimited within homogenous, distinct patches of *B. maritimus* and *P. australis* as is represented in Figure 4.



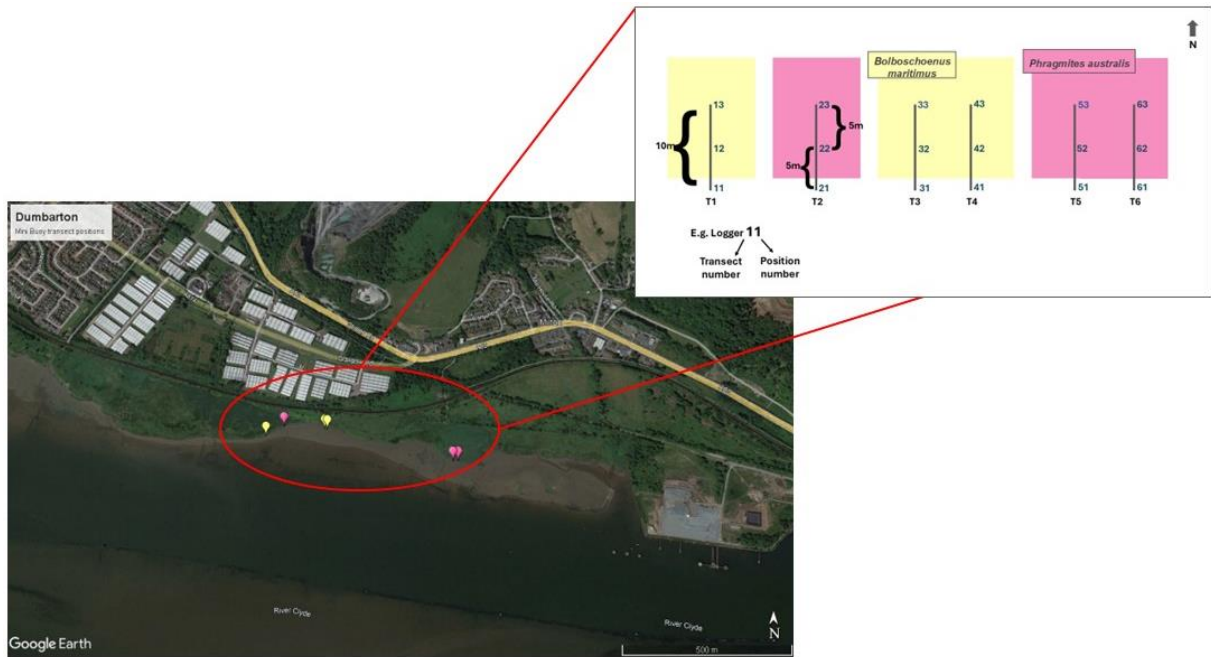


Figure 4. Layout of Mini Buoy logger deployment transects at the Dumbarton field site. Pendant and B4+ Mini Buoys were deployed 1m apart along each transect in parallel lines.

Transect 1 was furthest west and situated in a patch of *B. maritimus* which was bordered on its eastern side by a creek that separated it from the patch of *P. australis* that hosted transect 2 (Figure 4). Transects 3 and 4 were both *B. maritimus* transects; these transects were situated at the highest elevation compared to other transects in the study. The two transects furthest to the east were transects 5 and 6 and were both *P. australis* transects; these were situated at the lowest elevation compared to other transects in the study and were bordered on the eastern side by a creek (Figure 4). All these transects were within walking distance of each other at Dumbarton. This was convenient for fieldwork and allowed for the hydrodynamic and ecological data collected from these two species to be comparable by limiting the possibility of spatial variability in environmental conditions between the species sites. The field site at Dumbarton was also interesting due to its proximity to the town of Dumbarton. To the west of the field site, near Dumbarton Rock, housing developments are encroaching on the intertidal banks of the River Clyde. Infrastructure including warehouses and Glasgow Road closely border the saltmarsh at this site and, notably, the trainline from Glasgow to Balloch runs through the saltmarsh (Figure 5). The topic of flood defence is therefore especially pertinent at this site where infrastructure is imminently threatened.



Figure 5. Train line through saltmarshes in the Inner Clyde Estuary at Dumbarton.

## 3.2. Field Site Experimental Design

### 3.2.1. Effectiveness of two Mini Buoy models for the quantification of $C_v$ attenuation by vegetation

To examine which model is most effective at quantifying  $C_v$  attenuation, B4+ and Pendant Mini Buoys (Figure 6) were deployed 1m apart from each other in parallel lines with the first sensor tethered to the bare mudflat in front of the saltmarsh vegetation, one 5 m into the vegetation, and the last was positioned 10 m into the vegetation.

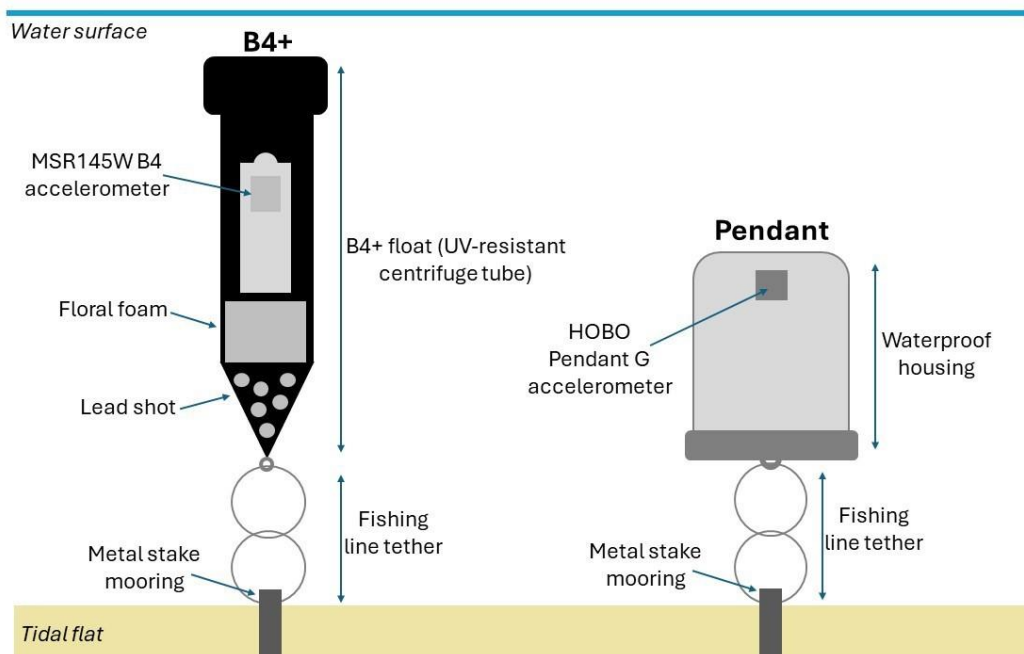


Figure 6. Representations of fully submerged B4+ and Pendant Mini Buoy models (figure adapted from Ladd et al. (2024)).

The B4+ model requires assemblage before deployment as the logger used for this model – the MSR145W B4 accelerometer (MSR Electronics GmbH, Switzerland; specifications in Table 2) – does not float well. The float, therefore, must be assembled and it consists of a sealed, UV-resistant centrifuge tube casing which contains lead shot, floral foam and the MSR145 accelerometer. The lead shot has proven to increase the sensitivity of the accelerometer to wave orbital velocity measurements by destabilising it in the water column due to reduced buoyancy (Ladd et al. 2024a), and the floral foam holds the logger in place within the tube. A hole is drilled at the bottom of the centrifuge tube so that a metal eye bolt can be inserted, this is covered in epoxy glue to waterproof it. To further waterproof the B4+, a rubber O-ring is inserted into the lid and the lid is then sealed by applying silicone sealant. Crimped fishing line rings are attached to the metal eye ring so that it can be securely tethered to a metal stake (Figure 6) but retain some freedom to move with the currents. The standard protocol for assembling the B4+ is described in detail in the Mini Buoy Handbook (Ladd et al. 2024b). The B4+ is 17 cm tall and should appear as in Figure 6 when fully assembled.

In contrast, the Pendant Mini Buoy model consists of the HOBO UA-004-64 Pendant G Acceleration Data Logger (specifications in Table 2) which is an integrated accelerometer and float. This model requires minimal assemblage before deployment as the housing of the data logger is waterproof and buoyant. Crimped fishing line rings need to be attached to the integrated anchor point so that it can be securely tethered to a metal rod but retain some freedom to move with the currents. The Pendant is ~11 cm tall and should appear as in Figure 6 when fully assembled.

The Mini Buoys deployed on the bare mudflat were anchored to the mudflat with the lower fishing line ring cable tied to a perforation at the top of a metal rod that has been hammered into the ground. To deploy the Mini Buoys within the vegetation canopy, an area of vegetation slightly greater than the height of the Mini Buoy itself – 25 cm<sup>2</sup> for the B4+ and 15 cm<sup>2</sup> for the Pendant – had to be cleared so that the movement of the Mini Buoy would not be restricted in any direction by the surrounding plants and impact the measurements recorded. A heavy, non-buoyant rubber mat was placed over the cleared vegetation to prevent it from growing back over the duration of the deployments. The rubber mat was anchored by pegs hammered through it and into the ground at each corner and the Mini Buoys were tethered to a metal rod that was hammered into the ground through a hole in the centre of the mat.

Table 2. Technical specifications for the HOBO UA-004-64 Pendant G and MSR145W B4 accelerometers.

	<b>HOBO UA-004-64 Pendant G</b>	<b>MSR145W B4</b>
Measurement range	±3g	±10 G / ±2 G selectable
Accuracy at 25oC	±0.075g	±0.15g
Memory	64K bytes	Formattable

For the purposes of this study, the Pendant loggers were set up to measure only x-axis acceleration at a frequency of 0.1Hz (one reading every 10 seconds). With these settings, the memory was filled within ~8 days after which the logger would stop recording. Pendant Mini Buoys were deployed for ~10 days at a time to minimise the gap in data between deployments. Throughout the duration of this study the batteries did not have to be changed in any of the Pendant Mini Buoys. The B4+ Mini Buoys were set up to measure only y-axis acceleration at a rate of 1Hz (one reading per second). With these settings the maximum duration of deployment for the logger was predicted to be 25 days after which the battery would run out of charge. The MSR 145 logger within the B4+ has an internal rechargeable battery so each deployment for the B4+ lasted ~20 days before being replaced by freshly programmed recharged ones. Three deployments of the B4+ Mini Buoys were carried out for this study. All loggers were first deployed on the 11<sup>th</sup> of May 2023 and in total, six deployments of the Pendant Mini Buoys and three deployments of the B4+ Mini Buoys were carried out. Between May 11<sup>th</sup> and August 1<sup>st</sup>, data for a total of 35.8 days was recorded by all Pendant Mini Buoys. Unlike the Pendant deployments there were no gaps between deployments for the B4+ Mini Buoys due to greater memory capacity (Table 2), therefore more data was collected in the same period by the B4+ sensors. A total of 51.6 days was recorded by the B4+ loggers on transects 1 to 5, and due to tidal conditions impacting logger retrieval on transect 6, a total of 54.7 days were recorded by the B4+ loggers on transect 6.

### 3.2.2. Assessment of plant traits for two saltmarsh species

The patches of *B. maritimus* and *P. australis* in which the Mini Buoys were deployed were monitored throughout the growing season from May to July. To assess plant and community characteristics of *B. maritimus* and *P. australis*, measurements of height, basal diameter and stem density were taken using the following protocol.

Quadrats of 1 m<sup>2</sup> were set up in the space between the two Mini Buoys models at each position along each transect. A 20 cm<sup>2</sup> subplot was set up in the top, right corner of the main quadrat. All species present in the quadrat were identified and the percentage cover for each was estimated by eye. The vegetation was reasonably homogenous so for more detailed measurements only the dominant species in the quadrat (either *B. maritimus* or

*P. australis*) was considered. All stems of the dominant species present in the subplot were counted and the height and basal diameter were measured for 10 live stems chosen randomly within the subplot. Plant height was measured using a tape measure from the ground to the tip of the plant. The basal diameter of the plants was measured using an electronic calliper at the stem ~2 cm from the ground. These measurements were taken every month from May to July; a total of three times over the monitoring period.

Plant trait measurements were used to derive vegetation parameters including: a) density ( $d$ , stems  $m^{-2}$ ), b) frontal surface area (FSA) calculated from plant height ( $h$ ), plant basal diameter ( $Bd$ ), and density as  $h \times Bd \times d$  (Figueroa-Alfaro et al. 2022) and, c) slenderness coefficient ( $S$ ), expressed as the ratio between stem basal diameter ( $Bd$ ) and stem height, where  $S = h/Bd$  (Chatagnier 2012; Vovides et al. 2014), which were further used to explore vegetation community characteristics and correlate plant traits with  $C_v$  attenuation capacity.

### 3.2.3. Assessment in $C_v$ attenuation between two saltmarsh species

In order to assess differences in current attenuation between two saltmarsh species,  $C_v$  was monitored on the mudflat and within the vegetation as outlined in section 3.2.1. so that attenuation could be quantified following the approach outlined in section 3.3.3. This was then correlated to the characteristic morphological traits of each species – *B. maritimus* or *P. australis* – following the approach outlined in section 3.3.3. Data on the characteristic morphological traits of each species was collected following the method outlines in section 3.2.2.

## 3.3. Statistical approach

### 3.3.1. Effectiveness of two Mini Buoy models for the quantification of $C_v$ attenuation by vegetation

To assess two models of the Mini Buoy – the B4+ and the Pendant – the inundation characteristics recorded by each model across the logger positions were calculated and compared. The percentage difference between the two models of the cumulative number of days recorded over the monitoring period was calculated to assess the practicality of each model as a long-term hydrodynamic monitoring device. To assess how differently inundation characteristics at the same site are represented by each model the percentage difference of the total recorded number of inundation events between them was calculated. Further, the total inundation duration detected by each model, represented as a percentage of the full monitoring duration, was calculated per logger position. Also, the total recorded number of inundations was divided by the total number of days monitored to gauge the number of inundations detected per day by each model at each logger position (mudflat, 5m vegetation, 10m vegetation) and the average number of inundations detected per day at each position was compared between loggers using a Wilcoxon test. Finally, to assess how effective each model was at detecting  $C_v$ , the number of inundation events with detectable  $C_v$  was calculated and represented as a

percentage of the total number of detected inundation events per model per logger position.

Due to the low percentage of inundation events with detectable  $C_v$  10m into the vegetation across both saltmarsh species, there was not enough  $C_v$  data available for a robust analysis of current attenuation 10m into the vegetation. Data from this logger position was therefore not used for  $C_v$  attenuation analyses in either *B. maritimus* or *P. australis*. Also, the B4+ recorded a lower percentage of inundation events with detectable  $C_v$  on the mudflat than the Pendant. The  $C_v$  data collected by the B4+ on the mudflat was not sufficient for a robust analysis of current attenuation therefore only data from the Pendant Mini Buoy model was used to assess  $C_v$  attenuation.

### 3.3.2. Assessment of plant traits for two saltmarsh species

To assess how each species behaved in relation to exposure to hydrodynamic energy, the slenderness ( $S$ ) of *B. maritimus* and *P. australis* was graphed over time separately for the vegetation developing at the mudflat and 5m into the vegetation and a Wilcoxon test was used to compare  $S$  means between the logger positions at each month for each species. Furthermore, to assess how vegetation characteristics changed over time and understand differences between species within the vegetation belt (at the point where current attenuation was measured), Wilcoxon test was used to compare FSA and density ( $d$ ) of each species 5m into the vegetation over the monitoring period within and between species over the monitoring period.

### 3.3.3. Assessing differences in $C_v$ attenuation between two saltmarsh species

Acceleration data from the Pendant Mini Buoy was used to calculate  $C_v$ . When fully inundated, any tilting of the Mini Buoy away from its vertical position ( $90^\circ$ ) in the water column is caused by the force of a current pushing against it where a greater tilt indicates a stronger current. Current velocity can be derived from the tilt of the Mini Buoy during full inundation according to calibrations carried out by Balke et al. (2021) and Ladd et al. (2024); these studies include a comprehensive description of the calibration of the Mini Buoys.

To assess current attenuation in *B. maritimus* and *P. australis*, the overall frequency of inundation events with detectable  $C_v$  (75<sup>th</sup> quantile value of inundation event greater than the HOB0 detection limit) over the entire monitoring period was calculated per species on the mudflat and 5m into the vegetation as an indicator of whether current attenuation was taking place. Further,  $C_v$  reduction was measured as the percentage reduction of the 75<sup>th</sup> quantile value of  $C_v$  measured by the Pendant Mini Buoy on the mudflat ( $I$ ) to the 75<sup>th</sup> quantile value of  $C_v$  measured by the Pendant 5m into the vegetation ( $V$ ) during the same inundation event:  $((I - V)/I) \times 100$ .

The average current reduction at *B. maritimus* and *P. australis* sites over the entire monitoring period were compared using a Wilcoxon test to determine whether there was

a significant difference between the two species. To investigate the temporal variability, the current reduction at each species site was plotted and compared between monitoring months (May, June, and July) using a Wilcoxon test. Further, to investigate how initial velocity ( $C_v$  at the mudflat) impacted current attenuation, the current reduction at each species site was sorted into inter-quartile bins according to their corresponding initial velocities ( $C_v$  measured at the mudflat position), and these bins were compared using Wilcoxon tests for each species.

Finally, three generalised additive models (GAMs) were run to investigate the impact of time, initial velocity, and either stem density, FSA, or slenderness on current attenuation in *B. maritimus* and *P. australis*. The most effective model for further analysis was identified by comparing the deviance explained by each model and the Akaike Information Criterion (AIC) for each model. The three generalised additive models (GAMs) were run each using saltmarsh species interactions with initial velocity, month, and either FSA (GAM1), density (GAM2), or slenderness (GAM3) as explanatory variables (smoothing terms), species was assigned as a fixed effect, and logger transect and position as random effects.

## 4. Results

### 4.1. Inundation characteristics

Table 3. Cumulative number of days recorded throughout the monitoring period by each Mini Buoy model at each transect.

Logger	Transects	Cumulative no. of days recorded
HOBO	1-6	35.8
MSR	1-5	51.6
	6	54.7
<b>Difference between HOBO and MSR (%)</b>		+44.13 - 52.80

The number of days recorded by the MSR Mini Buoy was overall higher than the number of days recorded by the HOBO Mini Buoy throughout the monitoring period of this study. The HOBO recorded a cumulative 35.8 days per transect over all the deployments (Table 3). The total duration of recording for the MSR on the other hand, was 44.13% - 52.80% higher than that of the HOBO at a cumulative 51.6 days of data from transects 1 to 5, and 54.7 days on transect 6 (Table 3).

#### 4.1.1. Number of inundation events

There was variation in the number of inundation events detected by each model at each logger position. At *P. australis* sites, the MSR detected a higher number of inundation events consistently across all logger positions (Table 4). At the mudflat for *P. australis*,

57.50% more events were detected by MSR than by HOBOS (Table 4) corresponding to the 44.13% - 52.80% greater duration recorded by MSR (Table 4). In contrast, 5m and 10m into the vegetation, numbers of inundation events detected by MSR compared to HOBOS were only increased by 25.17% and 5.38% respectively (Table 4). At *B. maritimus* sites, the number of inundation events detected by MSR was only greater than the number detected by HOBOS throughout the monitoring period on the mudflat, and this was only greater by 12.71% (Table 4). Within the vegetation at *B. maritimus* sites, the number of inundation events recorded by MSR was lower than the number recorded by HOBOS by 11.90% 5m into the vegetation and 28.89% 10m into the vegetation (Table 4).

Table 4. Number of inundation events recorded throughout the monitoring period by each Mini Buoy model per species.

Species	Logger position	Number of events		Difference between HOBO and MSR (%)
		HOBO	MSR	
<i>B. maritimus</i>	Mudflat	181	204	+12.71
	5m Veg.	126	111	-11.90
	10m Veg.	90	64	-28.89
<i>P. australis</i>	Mudflat	160	252	+57.50
	5m Veg.	151	189	+25.17
	10m Veg.	130	137	+5.38

Per day, the number of inundation events recorded by the MSR and HOBOS Mini Buoy models are not significantly different at the mudflat ( $p = 0.57$ ), 5m into the vegetation ( $p = 0.48$ ), or 10m into the vegetation ( $p = 0.065$ , Figure 7).

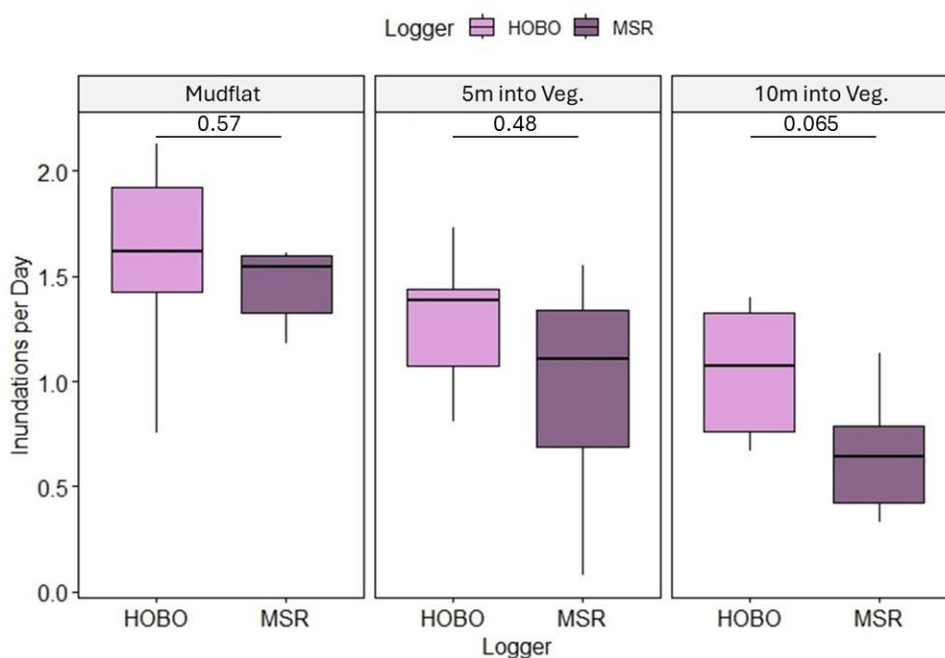


Figure 7. Boxplot depicting the number of inundation events recorded per day throughout the monitoring



period by each Mini Buoy model at each logger position. A Wilcoxon test is used to compare the logger models.

#### 4.1.2. Duration of inundation events

The total duration of all inundation events detected by HOBO loggers was greater than the duration detected by MSR loggers for all logger positions at *B. maritimus* sites and at all *P. australis* sites except for on the mudflat (Table 5). On the mudflat at *P. australis* sites, the total inundation duration detected by HOBOS amounted to 14.7% of the total recording time compared to the duration detected by MSRs was 16.9% of the total recording time.

Table 5. Total inundation duration detected per species and logger position expressed as a percentage of the full duration of recording per logger.

Species	Logger position	HOBO: Total inundation duration (%)	MSR: Total inundation duration (%)
<i>B. maritimus</i>	Mudflat	17.3	14.3
	5m Veg.	9.3	6.4
	10m Veg.	5.3	3.0
<i>P. australis</i>	Mudflat	14.7	16.9
	5m Veg.	11.9	10.2
	10m Veg.	9.2	7.1

#### 4.1.3. Number of inundation events with detectable currents

Inundation events with detectable  $C_v$  were recorded more frequently within the MSR dataset than within the HOBO dataset at *B. maritimus* sites 10m into the vegetation, and at *P. australis* sites both 5m and 10m into the vegetation (Table 6). However, on the mudflat for both species and 5m into the vegetation at *B. maritimus* sites, inundation events with detectable  $C_v$  were detected more frequently within the HOBO dataset than within the MSR dataset (Table 6).

Table 6. Inundation events with detectable currents expressed as a percentage of the total number of recorded inundation events (Table 4) per species and logger position.

Species	Logger position	Inundation events with detectable currents (%)	
		HOBO	MSR
<i>B. maritimus</i>	Mudflat	43.1	27.5
	5m Veg.	11.1	10.8
	10m Veg.	5.6	15.6
<i>P. australis</i>	Mudflat	21.3	19.8
	5m Veg.	13.9	25.9
	10m Veg.	2.3	14.6

## 4.2. Assessment of vegetation traits

### 4.2.1. Slenderness

Plants situated at the edge of the mudflat yielded relatively consistent slenderness values throughout growing season for both *B. maritimus* and *P. australis* (Figure 8). In contrast, a consistent increase in slenderness over the growing season was observed in plants located 5m into the vegetation for both species (Figure 8). Throughout the assessment period, a significant difference in slenderness can be observed between individuals at the edge of the mudflat and individuals 5m into the vegetation ( $p < 0.001$ ). In both *B. maritimus* and *P. australis* communities, higher average slenderness values were observed 5m into the vegetation consistently from May to August (Figure 8).

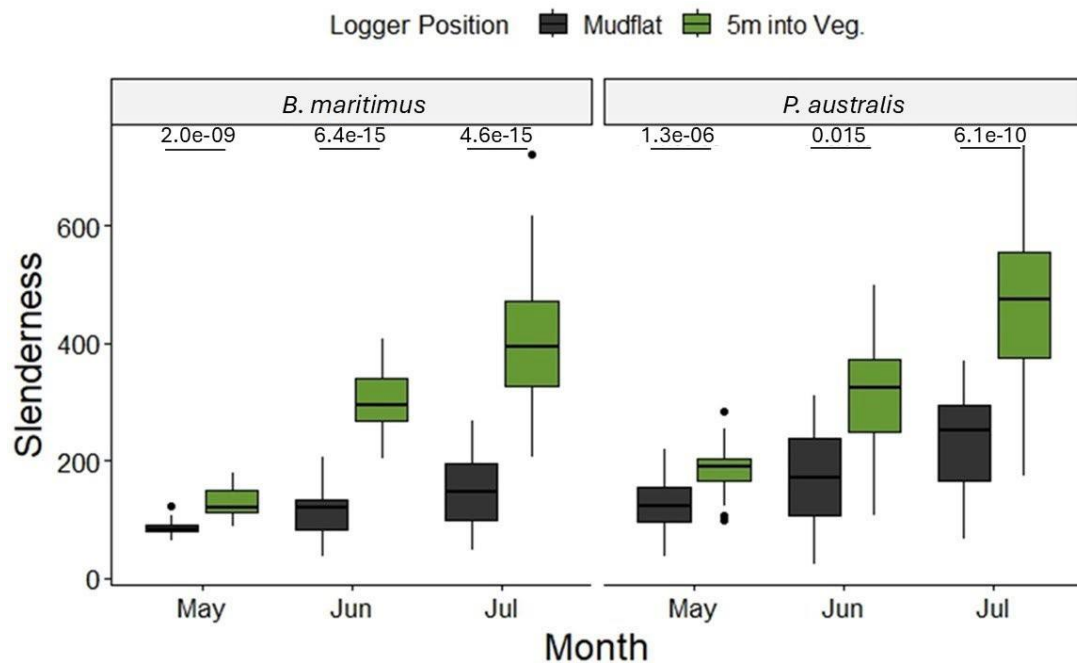


Figure 8. Boxplots depicting the change in the slenderness of *B. maritimus* and *P. australis*, respectively, over the growing season. Mean plant slenderness on the mudflat and 5m into the vegetation is compared with the Wilcoxon test.

### 4.2.2. Stem density

In *P. australis*, the density of living stems 5m into the vegetation was observed to change significantly over the growing season ( $p < 0.001$ ). Over the first two months from May to June, no significant change was observed in living stem density at *P. australis* sites ( $p = 0.058$ ). However, from June to July there was a significant increase in *P. australis* stem density ( $p < 0.001$ ) and an overall greater stem density was recorded at the end of the growing season than at the start ( $p < 0.001$ ). At the *B. maritimus* sites, 5m into vegetation, no significant change in living stem density was measured between months from May to June ( $p = 0.63$ ) or from June to July ( $p = 0.14$ ), or over the entire monitoring period ( $p = 0.93$ ) (Figure 9A).

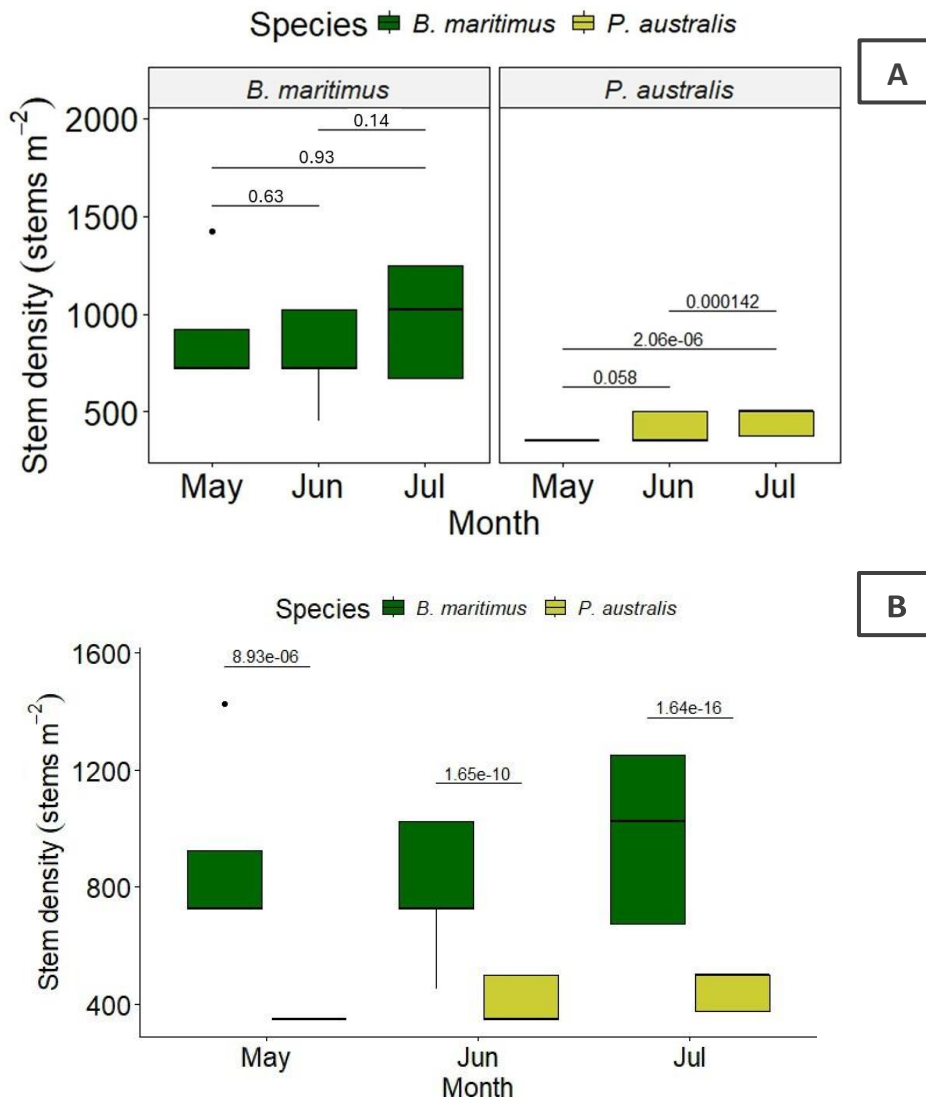


Figure 9. Boxplots depicting the change in stem density of *B. maritimus* and *P. australis* over the growing season 5m into the vegetation. A) the change in mean stem density over time within each species respectively is compared with the Wilcoxon test. B) the mean stem densities of *B. maritimus* and *P. australis* over the growing season are compared to each other with the Wilcoxon test.

Significant differences in live stem density were observed throughout the season between *B. maritimus* and *P. australis* ( $p < 0.001$ ; Figure 9B). Observations every month over the monitoring period indicated that *B. maritimus* stem densities were consistently higher than that of *P. australis* in May ( $p < 0.001$ ), in June ( $p < 0.001$ ), and in July ( $p < 0.001$ ) (Figure 9B).

#### 4.2.3. Frontal surface area

The frontal surface area (FSA) 5m into the vegetation at both *P. australis* and *B. maritimus* stands increased significantly throughout the growing season ( $p < 0.001$ ; Figure 10A). Also, *B. maritimus* FSA was consistently higher than that of *P. australis* in May ( $p < 0.001$ ), in June ( $p < 0.001$ ), and in July ( $p < 0.001$ ) (Figure 10B).

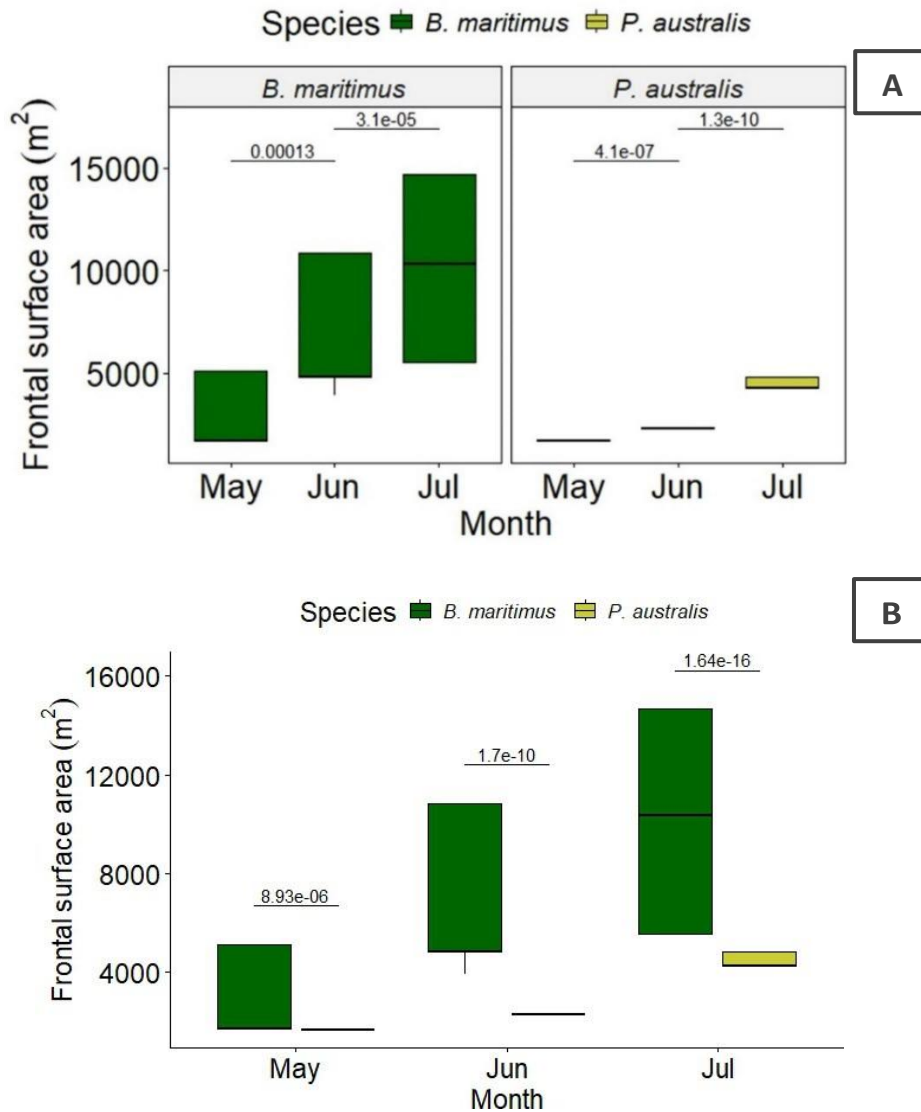


Figure 10. Boxplots depicting the change in frontal surface area of *B. maritimus* and *P. australis* over the growing season 5m into the vegetation. **A)** the change in mean frontal surface area over time within each species respectively is compared with the Wilcoxon test **B)** the mean frontal surface areas of *B. maritimus* and *P. australis* over the growing season are compared to each other with the Wilcoxon test.

### 4.3. Current velocity ( $C_v$ ) attenuation

#### 4.3.1. Difference between species

The frequency of inundation events with detectable  $C_v$  throughout the monitoring period was higher on the mudflat than it was 5m into the vegetation for both *B. maritimus* and *P. australis* (Figure 11). At *B. maritimus* sites the frequency of inundation events with detectable  $C_v$  was 46.7% on the mudflat and 9.2% 5m into the vegetation, a difference of 37.5% (Figure 11). At *P. australis* sites the frequency of inundation events with detectable  $C_v$  was 21.0% on the mudflat and 16.0% 5m into the vegetation; a difference of 5% (Figure 11).

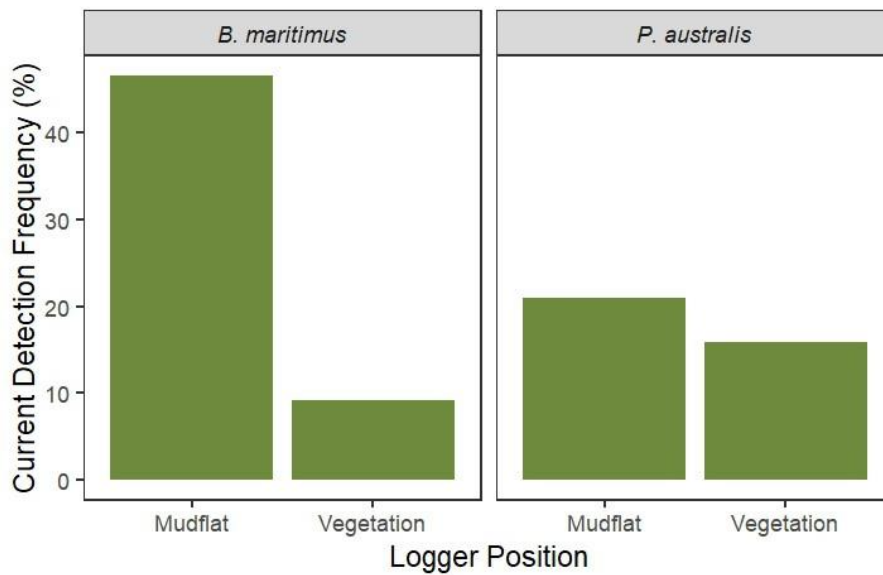


Figure 11. Frequency of inundation events with detectable  $C_v$  (75th quantile value of inundation event greater than the HOBO logger detection limit) depicted as a percentage of all full inundation events detected across mudflat and vegetation logger positions for *B. maritimus* and *P. australis* respectively.

The difference between percentage frequency of events with detectable inundations at the mudflat and 5m into the vegetation is 32.5% greater at *B. maritimus* sites (37.5%) than at *P. australis* sites (5%). On the mudflat, inundation events with detectable  $C_v$  velocities were 25.7% higher at *B. maritimus* sites than at *P. australis* sites (Figure 11). However, 5m into the vegetation, the frequency of inundation events with detectable  $C_v$  was 6.8% higher for *P. australis* sites than for those of *B. maritimus* (Figure 11).

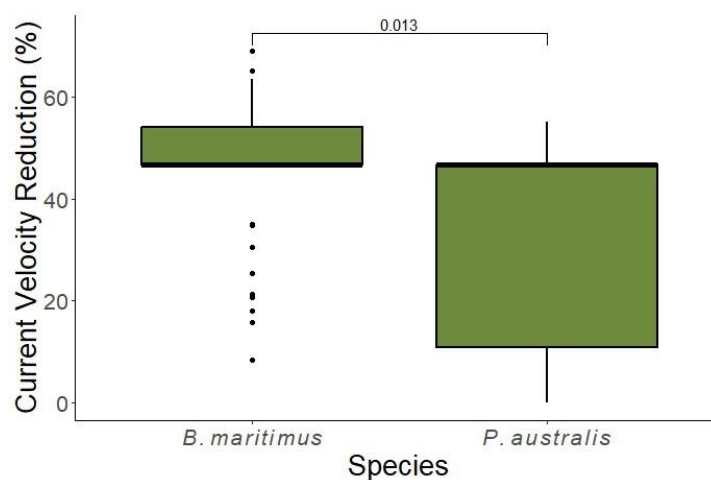


Figure 12.  $C_v$  reduction observed in *B. maritimus* and *P. australis* over the whole monitoring period compared using a Wilcoxon test.

Reduction of  $C_v$  within the canopy was detected at both *B. maritimus* and *P. australis* sites (Figure 12). Overall, the mean percentage reduction of  $C_v$  within the canopy of *B. maritimus* was greater ( $p = 0.013$ ) than that within the canopy of *P. australis* (Figure 12). The maximum  $C_v$  attenuation detected within the *B. maritimus* canopy was 69.01%, within the *P. australis* canopy the maximum  $C_v$  attenuation detected was 55.06% (Figure 12).

When plotted over time, the mean reduction in  $C_v$  did not change significantly over time for either *B. maritimus* ( $p = 0.078$  from May to June;  $p = 0.61$  from June to July) or *P. australis* ( $p = 0.43$  from June to July) (Figure 13) though greater variation in current reduction was observed in July for both. No data points were available for *P. australis* in May (Figure 13).

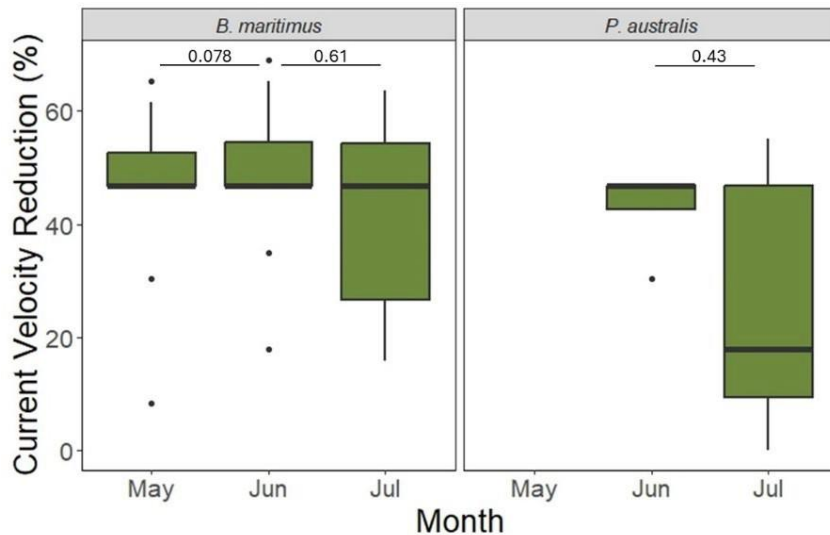


Figure 13.  $C_v$  reduction observed per month in *B. maritimus* and *P. australis*, respectively, compared using a Wilcoxon test.

When plotted against the initial  $C_v$  detected on the mudflat, a significant effect on current reduction was observed in *B. maritimus* (Figure 14).  $C_v$  reduction in both species was plotted against initial  $C_v$  on the mudflat in bins according to their respective inter-quartile ranges and above the HOBO detection limit ( $0.049 \text{ ms}^{-1}$ ). In the case of *B. maritimus*, a significant increase in mean current reduction was observed between bins as initial  $C_v$  increased ( $p < 0.001$ ) up to a maximum of  $0.16 \text{ ms}^{-1}$  (Figure 14).

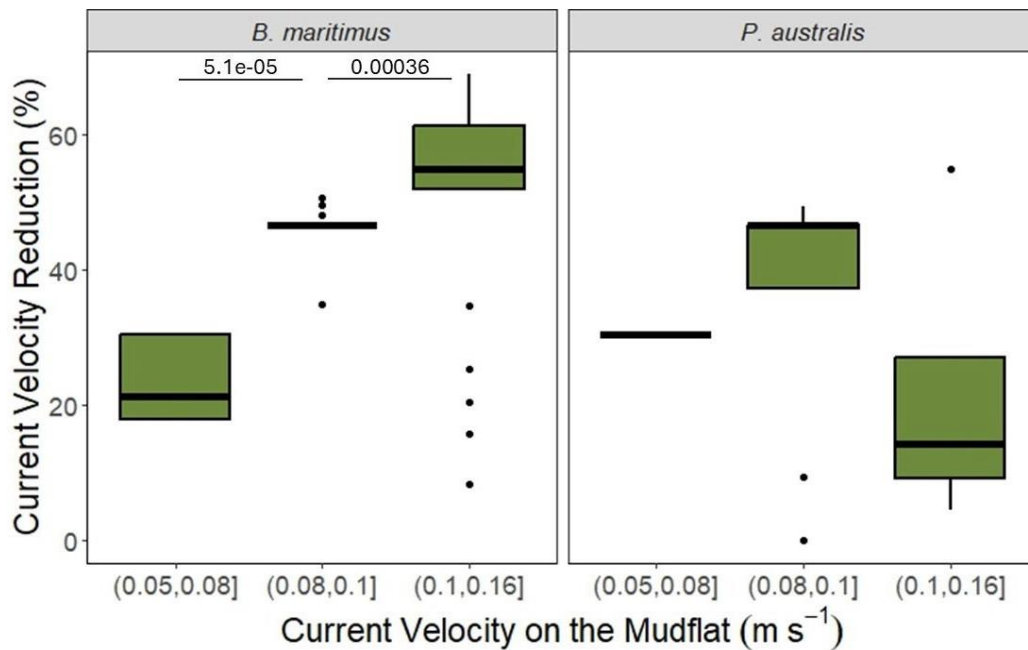


Figure 14. Boxplots depicting the Cv reduction per species in response to initial Cv represented in inter-quartile bins.

In the case of *P. australis*, no clear pattern in current reduction emerged between the inter-quartile range bins (Figure 14). A Wilcox test could not be carried out between the bins for *P. australis* because there were not enough observations in each bin; only 13 inundations with detectable currents at both logger positions on the transects were recorded by HOBO loggers at *P. australis* sites throughout the monitoring period. The maximum initial Cv recorded at the *P. australis* site was 0.12 ms<sup>-1</sup>.

#### 4.3.2. Effect of plant traits on Cv attenuation

Table 7. Summary of outcomes (deviance explained by the model and AIC) of three generalised additive models run on the HOBO data.

Models	Veg. parameter	Deviance explained	AIC
GAM1	FSA	81.2%	228.13
GAM2	Density	82%	229.86
GAM3	Slenderness	81.2%	228.20

Three generalised additive models (GAMs) were run each using saltmarsh species interactions with initial velocity, month, and either FSA (GAM1), density (GAM2), or slenderness (GAM3) as explanatory variables (smoothing terms), species as a fixed effect, and logger transect and position as random effects. Each of the models tested different vegetation parameters as an explanatory variable (Table 7). Of the three GAMs, the deviance explained by GAM2 was the highest at 82% though the deviance explained by the models differed by less than 1% overall (Table 7). However, GAM1 had the smallest AIC denoting the best fit though the overall difference between the models was smaller than 2 (Table 7).

Of the three vegetation parameters tested as explanatory variables, only the stem density

(GAM2) of *B. maritimus* was found to have a significant impact on current attenuation ( $p = 0.035$ ,  $df = 3$ ), while stem density (GAM2) of *P. australis* was not found to have any significant impact on current attenuation ( $p = 0.45$ ,  $df = 3$ ). GAM1 found that FSA had no significant impact on the current reduction in either *B. maritimus* ( $p = 0.17$ ,  $df = 3$ ) or *P. australis* ( $p = 0.70$ ,  $df = 3$ ) and GAM3 found that Slenderness had no significant impact on the current reduction in either *B. maritimus* ( $p = 0.08$ ,  $df = 3$ ) or *P. australis* ( $p = 0.60$ ,  $df = 3$ ).

Since the differences in AIC were not significant between the three models tested and GAM2 had the highest explanatory power (82%, Table 7) and observed a significant relationship between an attribute of the vegetation (stem density) and current attention, GAM2 was chosen for further exploration.

GAM2 found no significant relationship between monitoring month and current reduction in either *B. maritimus* ( $p = 0.91$ ,  $df = 3$ ) or *P. australis* ( $p = 0.45$ ,  $df = 3$ ).

Stem density was found to significantly impact current attenuation in the case of *B. maritimus* ( $p = 0.035$ ,  $df = 3$ ). Current attenuation capacity in response to stem density was found to steadily increase with increasing stem density until reaching a maximum at ~38% current reduction at a stem density of 750 stems  $m^{-1}$  (Figure 15A). At stem densities higher than 750 stems  $m^{-1}$ , current reduction decreases as stem densities increase. For *P. australis*, no significant effect of stem density on current reduction was observed ( $p = 0.45$ ,  $df = 3$ ).

Current attenuation changed significantly in response to initial  $C_v$  in both *B. maritimus* ( $p < 0.001$ ,  $df = 3$ ) and *P. australis* ( $p = 0.001$ ,  $df = 3$ ). For *P. australis*, current attenuation capacity increases as initial  $C_v$  increases until a peak of just over 40% current reduction at an initial  $C_v$  of ~0.095  $ms^{-1}$  (Figure 15B). The model predicts two peaks for *B. maritimus* (Figure 15B). The current attenuation capacity of *B. maritimus* increases steadily to an initial peak of almost 50% current reduction at an initial  $C_v$  of ~0.095  $ms^{-1}$  (Figure 15B) after which it falls until a trough of ~40% current reduction between 0.10-0.11  $ms^{-1}$  (Figure 15B). The attenuation capacity of *B. maritimus* is observed to increase again steadily in response to initial  $C_v$  to its overall maximum at ~60% current reduction at an initial velocity of ~0.13  $ms^{-1}$  (Figure 15B).



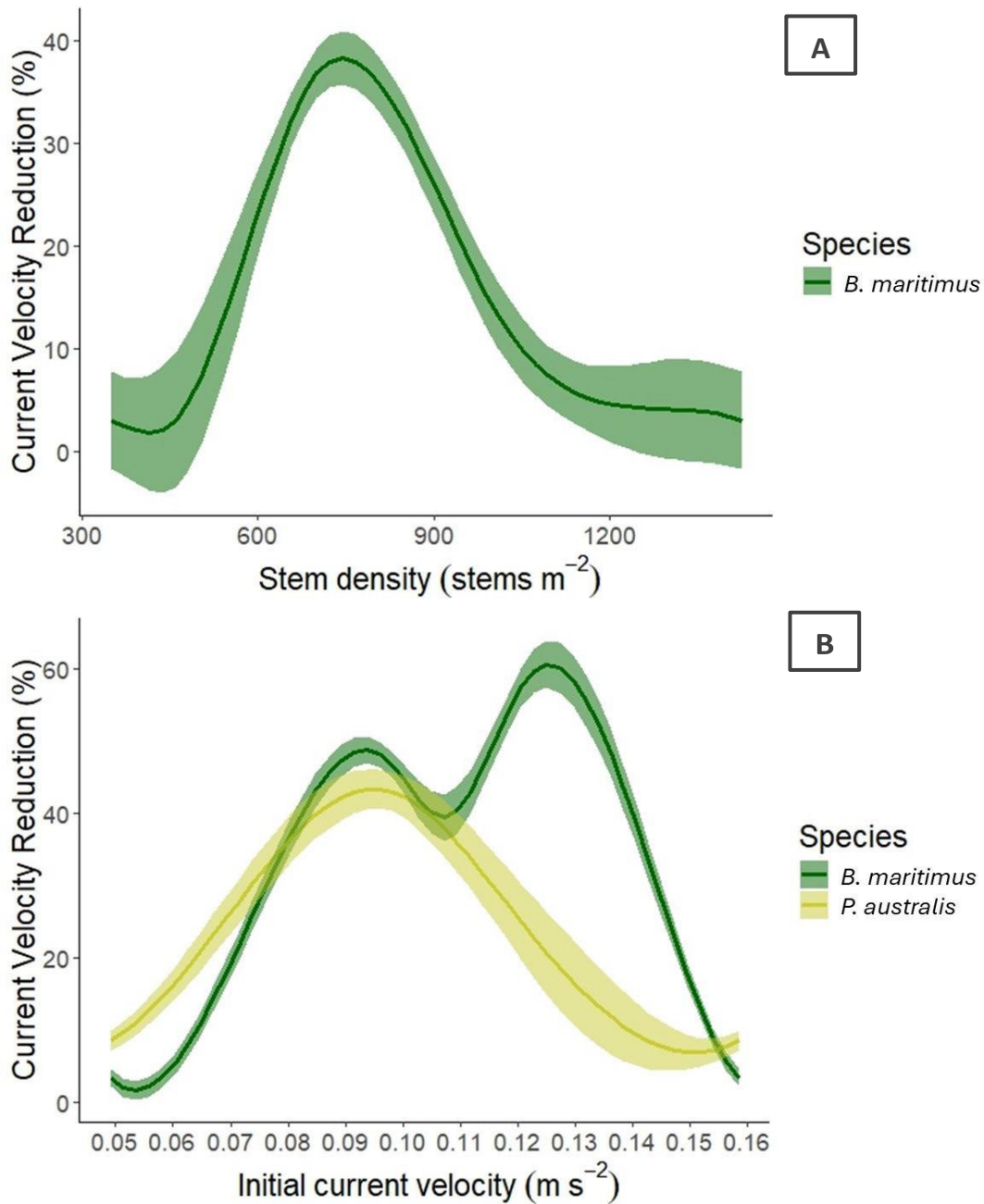


Figure 15. Generalised additive model (GAM2) showing how current reduction (%) by two saltmarsh species, *B. maritimus* and *P. australis*, is impacted by **A)** stem density and **B)** initial Cv. Initial Cv, stem density, and sampling month were used as smoothing terms, logger transect and position as random effects, and species as a fixed effect. The solid lines represent fitted values while the envelopes represent the standard error.

## 5. Discussion

### 5.1. Effectiveness of two mini buoy models in quantifying $C_v$ attenuation inside vegetation

The results of this study suggest that both the MSR and the HOBO Mini Buoy produce similar results for detecting the number of tidal inundations, but that the HOBO may be more effective for deriving inundation durations in shallower environments. Inundations per day that each model of the Mini Buoy detected did not differ significantly (Figure 7) at any of the logger positions suggesting that both the HOBO and MSR are equally effective for determining this parameter. However, the HOBO Mini Buoy consistently measured longer inundations than the MSR at all logger positions except for on the mudflat at *P. australis* sites (Table 5). Because the starting point of an inundation is informed by a threshold tilt of the logger, and the HOBO is a smaller model that requires less water depth for full inundation, the HOBO can start detecting inundations before MSRs at the same elevation. HOBOs therefore provide a more accurate representation of inundation durations, especially in environments with generally shallow inundations (such as higher up and further inland in inter-tidal habitats). The lowest-elevation sites in this study were *P. australis* sites on the mudflat, which were the only logger positions where the inundation durations measured by MSRs was longer than those measured by HOBOs (Table 5). The difference however was only of about 2.2% (Table 5) which could be due to freshwater inputs observed from creeks adjacent to *P. australis* sites and the low elevation of the mudflat site causing possible waterlogging and water levels rising faster here relative to other sites. Further studies comparing the two Mini Buoy models could help determine whether they detect inundation duration more equitably at low-elevation sites and how the rate of tidal inundation can have an impact.

For detecting and quantifying current attenuation in this study, the HOBO Mini Buoy was overall more effective. Tidal inundations with  $C_v$  above the detection limit of the Mini Buoys at multiple points along the transect were required to quantify  $C_v$  reduction. Records from logger positions 10m into the vegetation at both *B. maritimus* and *P. australis* sites were not used for analysis after initial exploration of the data because the numbers of inundations with detectable  $C_v$  recorded there were too low (Table 6) to provide robust results. Similarly, the numbers of inundations with detectable  $C_v$  recorded by the MSR on the mudflat were too low (Table 6) to provide robust results.  $C_v$  on the mudflat provided a benchmark from which current reduction within the vegetation could be measured; for both species, the number of inundation events with detectable  $C_v$  detected by the MSR was lower than that detected by the HOBO (Table 6). This was despite the MSR model's lower detection limit (MSR,  $0.018 \text{ ms}^{-1}$ ; HOBO,  $0.049 \text{ ms}^{-1}$ ) and could be due to the differences between the heights of the models.

The Mini Buoys must be fully inundated and upright in the water column to begin measuring  $C_v$ . As the HOBO is a shorter model, it will reach full inundation more often than the MSR, become fully inundated before the MSR, and stay fully inundated after the MSR within the same inundation event and stay inundated for an overall longer duration during each inundation event. The HOBO can reach full inundation more often than the MSR for example during neap tides when water depth is too shallow for the MSR to be fully inundated. This and staying fully inundated for longer periods of time than the MSR allow the HOBO to collect more datapoints both over different inundation events and during a single event. Also, reaching full inundation more quickly than the MSR as the tide comes in and remaining fully inundated for longer than the MSR as the tide ebbs, allows the HOBO to collect more datapoints during the flood and ebb tide periods when high  $C_v$  was experienced at this site. A larger proportion of the time for which the MSR is fully inundated and able to measure  $C_v$  is during slack tide when the water is unstressed. The MSR might therefore be better suited to detecting  $C_v$  attenuation at sites that experience deeper inundations or greater tidal amplitudes where tides can come in faster; this can be tested in further studies.

In terms of practicality, the B4+ is more convenient for long-term deployment and could collect data at a higher frequency but the Pendant was observed to be more durable and less destructive when deployed within the vegetation. Deployments of the B4+ in this study lasted up to 26 days with measurements taken at a rate of 1Hz while the Pendant, even at a lower measurement rate of 0.1Hz, could only record continuously for ~7.5 days. This meant that two Pendant deployments were necessary to capture a full tidal cycle of ~15 days as is recommended for analysis (Ladd et al. 2024a; Ladd et al. 2024b), and that even with loggers being replaced as often as possible (every ~10 days) there would be a gap of a few days in the dataset consistently between deployments. However, the Pendant is much more practical to assemble than the B4+ and throughout the duration of this study, none of the Pendant loggers were damaged which would be well suited for higher-energy sites. The B4+ loggers took at least 24 h to assemble and were susceptible to damage such as cracking of the centrifuge tube or insufficient waterproofing causing data to be unusable in these instances. Furthermore, as a smaller Mini-Buoy, the Pendant required that only a 15 cm<sup>2</sup> area of vegetation had to be cleared for its deployment within the vegetation whereas the B4+ required 25 cm<sup>2</sup>. This amounted to significantly greater damage to the vegetation for the deployment of the B4+ over the 6 transects for this study.

HOBO was overall more effective than the MSR for quantifying  $C_v$  attenuation by the saltmarsh vegetation in this study where the field site on the Inner Clyde Estuary was generally low energy with shallow inundations. Practically, though the B4+ is better suited to long-term deployments, this site was easily accessible so the Pendant could be regularly replaced the Pendant was the better suited for deployment within the vegetation as it caused less damage to the vegetation. Replication of this model comparison across different intertidal environments will help determine if the HOBO remains the better

suited model for  $C_v$  quantification under different physical conditions such as different tidal amplitudes, rates of incoming tides, and depths of inundations.

## 5.2. Plant traits of two saltmarsh species and their role in effective $C_v$ attenuation

Differing patterns of plant growth on the mudflat and within the vegetation for both *B. maritimus* and *P. australis*, as shown by differences in slenderness (Figure 8), could be an effect of flow stress on the community. The mechanical stability to withstand near-constant flow stress is essential to plants inhabiting inter-tidal areas. Studies have shown that plants can exhibit morphological changes to adapt to flow stress (Puijalon et al. 2005, 2008) which could explain the decreased slenderness observed at the vegetation edge (mudflat) as compared to 5m into the vegetation for both species. Lower slenderness values at the vegetation edge that do not increase greatly over the season suggest that plants growing here prioritise maintaining thicker stems which, as proposed by Carus et al. (2016), could be an adaptive response to exposure to higher  $C_v$  as thicker plants are better able to withstand these currents without mechanical failure. In contrast, the significant increase in slenderness values for both *B. maritimus* and *P. australis* over the season 5m into the vegetation suggests that individuals sheltered within the vegetation belt are prioritising height over diameter. These findings support that plants can exhibit morphological changes in response to flow stress and suggest that both *B. maritimus* and *P. australis* are allocating resources differently in response to flow stress. This self-adaptive ability increases the resistance capacity of the whole vegetation community to flow stress as sturdier plants at the vegetation edge can shelter individuals further within the belt against  $C_v$ . This community characteristic helps *B. maritimus* and *P. australis* survive and persist in the pioneer zone. This morphological adaptation could also have benefits for the attenuation and self-regulation capacity of nature-based coastal defences.

However, while both *B. maritimus* and *P. australis* were observed growing in the pioneer zone in the Inner Clyde Estuary, *P. australis* was observed to develop at sites exposed to lower hydrodynamic energy. Inundation events with detectable  $C_v$  were over twice as frequent on the mudflat at *B. maritimus* sites as compared to *P. australis* sites and the maximum initial  $C_v$  at *P. australis* was  $0.12 \text{ ms}^{-2}$  compared to  $0.16 \text{ ms}^{-2}$  at *B. maritimus*. Therefore, *P. australis* may be more sensitive to hydrodynamic forcing which can be associated with the significant morphological differences between the *B. maritimus* and *P. australis* communities in terms of frontal surface area (FSA) and stem density. Though the FSA and stem density of *P. australis* increased over the growing season, both FSA and stem density were consistently much higher in *B. maritimus*. As FSA or stem density increase, rates of hydrodynamic energy attenuation are also expected to increase (Figueroa-Alfaro et al. 2022) which would increase the ability of the entire vegetation belt to resist flow velocities and persist at an exposed site. Therefore, despite exhibiting the

same self-adaptive morphological capacity as *B. maritimus*, these findings suggest that the magnitude of flow stress that *P. australis* can withstand is comparatively lower due to its lower FSA and stem density. Differing sensitivity to hydrodynamic forcing between saltmarsh species should be considered in ecosystem management decisions, especially for nature-based flood defence.

### 5.3. Differences in current attenuation between two saltmarsh species

The findings of this study confirm that attenuation of  $C_v$  within saltmarsh vegetation is occurring in the Inner Clyde estuary. The frequency of inundation events with detectable  $C_v$  decreased from the mudflat to 5m into the saltmarsh vegetation for both *B. maritimus* and *P. australis* (Figure 11) indicating that some attenuation was occurring. Current reduction was observed up to 69.01% (Figure 12) of the initial  $C_v$  during this study at the Inner Clyde Estuary.

Contrary to previous studies which had observed that an increased rate of attenuation in response to increased frontal surface area (FSA) (Figueroa-Alfaro et al. 2022; Mendez & Losada 2004), this study found that FSA had no significant impact on current attenuation. This study also found that stem slenderness also did not have any direct significant impacts on current attenuation despite being an indicator of mechanical stability. However, stem density did have a significant impact on current attenuation in this study, but only in *B. maritimus*, and – as the stem density of *B. maritimus* did not change significantly throughout the study period (Figure 9A) - this did not indicate any temporal variability in attenuation capacity in the vegetation. This study also found no significant relationship between monitoring month and current reduction in either *B. maritimus* ( $p = 0.91$ ,  $df = 3$ ) or *P. australis* ( $p = 0.45$ ,  $df = 3$ ). This was contrary to findings by Möller & Spencer (2002) who observed seasonal changes in current attenuation which were positively correlated with seasonal changes in vegetation density. It is possible that the length of the monitoring period for this study was not sufficient to capture the impact of seasonality. The dataset used by Möller & Spencer (2002) spanned a year and only found differences between seasons whereas the dataset used for this study only spanned one season from May to July. A study monitoring hydrodynamics and correlating them with FSA, stem density, and slenderness at four different points of the year in different seasons might provide a better insight into the temporal variability of the attenuation capacity of the saltmarsh communities in the Inner Clyde Estuary.

The impact of *B. maritimus* stem density on current attenuation produces a nonlinear relationship wherein an intermediate stem density attenuates  $C_v$  most effectively (Figure 15A). A possible cause of this observed pattern was presented in a study by Harley & Bertness (1996) which found that increased crowding in saltmarsh plants (plants growing in areas of high stem density) was positively correlated with plant slenderness and negatively correlated with resilience to mechanical stress. This would suggest that there may be a threshold stem density of *B. maritimus* beyond which increasing stem density

is not beneficial for current attenuation. This pattern is also reflected by a similar nonlinear relationship Xu et al. (2022) found between stem density and sediment deposition in saltmarshes where attenuation of hydrodynamic energy by vegetation is known to encourage sediment to settle on the marsh. Furthermore, to explore the cause of the intermediate dip in current attenuation capacity for *B. maritimus* (Figure 15B), the temporal variability of vegetation growth and  $C_v$  on the mudflat, and the impact this has on attenuation capacity in response to initial  $C_v$ , should be further studied. Further investigations into the causes of spatial and temporal variability in *B. maritimus* stem density and corresponding hydrodynamic conditions will be important in understanding what creates this nonlinear relationship. Importantly, this would have implications for the use of *B. maritimus* in nature-based flood mitigation planning.

Overall, a significant difference in hydrodynamic energy attenuation capacity between *B. maritimus* and *P. australis* was observed. At the mudflat inundation events with detectable  $C_v$  were over twice as frequent at *B. maritimus* sites as compared to *P. australis* sites and frequencies reduced for both further into the vegetation, but inundation events with detectable  $C_v$  5m into the vegetation were more frequent at *P. australis* sites than at *B. maritimus* sites. The reduction in frequency of inundation events with detectable  $C_v$  between the mudflat and 5m into the vegetation was therefore greater in *B. maritimus* than in *P. australis*. The reduction in frequency of inundation events with detectable  $C_v$  5m into vegetation indicates some current attenuation in both species. However, the greater reduction in frequency observed in *B. maritimus* suggests that this species has a greater attenuation capacity. This is supported by the observed magnitudes of current attenuation between the two species where *B. maritimus* was found to reduce  $C_v$  by significantly more ( $p = 0.013$ ) than *P. australis* overall.

The results of GAM2 also supported that *B. maritimus* is more effective at attenuating currents than *P. australis*. A nonlinear relationship was observed between initial  $C_v$  and current reduction in both species. The maximum current attenuation was observed at an intermediate initial  $C_v$  value for both species as well (Figure 15B). At initial  $C_v$  below  $0.08 \text{ ms}^{-2}$ , greater current reduction by *P. australis* was observed in this study (Figure 15B). However, beyond this point, current reduction by *B. maritimus* remains consistently greater than that of that *P. australis* (Figure 15B). Even where *P. australis* reached a maximum current reduction of just over 40% at an initial velocity of  $\sim 0.095 \text{ ms}^{-2}$ , *B. maritimus* had the capacity to reduce  $C_v$  by almost 50% at the same point. Also, the maximum current attenuation of *B. maritimus* was much higher at  $\sim 60\%$ , and this was observed at a higher initial  $C_v$  of  $\sim 0.125 \text{ ms}^{-2}$  (Figure 15B). *B. maritimus* therefore demonstrated overall greater current reduction potential at a higher initial  $C_v$  than did *P. australis* (Figure 15B) in the environment of the Inner Clyde Estuary.

## 6. Conclusions

The Pendant Mini Buoy was more effective than the B4+ for quantifying  $C_v$  attenuation by the saltmarsh vegetation in the Inner Clyde Estuary, a low energy site with shallow inundations. The Pendant Mini buoy was also less destructive when deployed within the vegetation and more durable than the B4+. However, the B4+ is the better model for long-term deployments. Both models of the Mini Buoy were equally effective at measuring inundation characteristics in this study. The Pendant is therefore the recommended Mini Buoy model for deployment within saltmarsh vegetation for future studies. However, the drawback of its significantly shorter deployment times is important to consider in the experimental design. To further develop the use of the Mini Buoy for monitoring hydrodynamics within coastal vegetation, further studies comparing the use of different models of the Mini Buoy in other coastal environments (e.g. mangroves, seagrass beds) or sites with other inundation characteristics should be conducted to assess suitability.

Morphological adaptations to the physical environment were observed in both *B. maritimus* and *P. australis* where slenderness increased significantly between plants on the wave-exposed seaward boundary and those sheltered 5m into the vegetation for both species. This finding contributes to our understanding of how biophysical interactions on saltmarshes impact plant physiology. These physiological adaptations will, in turn, impact ecosystem service delivery including hydrodynamic energy attenuation. Therefore, further studies should be conducted that focus on understanding biotic adaptive responses to physical conditions as this is essential for predicting the long-term viability of nature-based coastal defences especially under rapidly changing conditions due to climate change.

Moreover, though both *B. maritimus* and *P. australis* were found in the pioneer zone in the Inner Clyde Estuary, *P. australis* was found at lower-energy sites compared to *B. maritimus* suggesting that *P. australis* is more sensitive to hydrodynamic forcing. This could be associated with the significant morphological differences observed between *B. maritimus* and *P. australis* throughout the growing season with higher FSA and density consistently observed in *B. maritimus*. Furthermore, *B. maritimus* with a maximum  $C_v$  attenuation of ~60%, was found to be overall more effective at attenuating  $C_v$  than *P. australis* which attenuated  $C_v$  to a maximum of ~40%. These findings provide an insight into the existing hydrodynamic energy attenuation potential of saltmarsh vegetation in the Inner Clyde Estuary and have important implications for the management of this area with the long-term goal of sustainable solutions for flood management in mind.

## 7. Bibliography

- Abraham A, Sommerhalder K, Abel T (2010) Landscape and well-being: A scoping study on the health-promoting impact of outdoor environments. *International Journal of Public Health* 55:59–69
- Adams JB, Raw JL, Riddin T, Wasserman J, Van Niekerk L (2021) Salt marsh restoration for the provision of multiple ecosystem services. *Diversity* 13:680
- Allen JRL (2000) Morphodynamics of Holocene salt marshes: a review sketch from the Atlantic and Southern North Sea coasts of Europe. *Quaternary Science Reviews* 19:1155–1231
- Augustin LN, Irish JL, Lynett P (2009) Laboratory and numerical studies of wave damping by emergent and near-emergent wetland vegetation. *Coastal Engineering* 56:332–340
- Balke T, Herman PMJ, Bouma TJ (2014) Critical transitions in disturbance-driven ecosystems: identifying Windows of Opportunity for recovery. *Journal of Ecology* 102:700–708
- Balke T, Stock M, Jensen K, Bouma TJ, Kleyer M (2016) A global analysis of the seaward salt marsh extent: The importance of tidal range. *Water Resources Research* 52:3775–3786
- Balke T, Vovides A, Schwarz C, L. Chmura G, Ladd C, Basyuni M (2021) Monitoring tidal hydrology in coastal wetlands with the ‘mini Buoy’: Applications for mangrove restoration. *Hydrology and Earth System Sciences* 25:1229–1244
- Barbier EB, Hacker SD, Kennedy C, Koch EW, Stier AC, Silliman BR (2011) The value of estuarine and coastal ecosystem services. *Ecological Monographs* 81:169–193
- Basyuni M, Amelia R, Suryanto D, Susetya IE, Bimantara Y (2022) Empowerment of Abandoned Ponds for Sustainable Mangrove Rehabilitation Activities in Percut Sei Tuan, Deli Serdang, Indonesia. *Journal of Sylva Indonesiana* 5:137–147
- De Battisti D, Fowler MS, Jenkins SR, Skov MW, Rossi M, Bouma TJ, Neyland PJ, Griffin JN (2019) Intraspecific root trait variability along environmental gradients affects salt marsh resistance to lateral erosion. *Frontiers in Ecology and Evolution* 7:1-11
- Beaumont NJ, Jones L, Garbutt A, Hansom JD, Toberman M (2014) The value of carbon sequestration and storage in coastal habitats. *Estuarine, Coastal and Shelf Science* 137:32–40
- Bekic D, Ervine DA, Lardet P (2006) A comparison of one- and two-dimensional model simulation of the Clyde Estuary, Glasgow. Philadelphia



- Bertness MD, Ewanchuk PJ, Silliman BR (2002) Anthropogenic modification of New England salt marsh landscapes. *Proceedings of the National Academy of Sciences* 99:1395–1398
- Billah MM, Bhuiyan MKA, Islam MA, Das J, Hoque AR (2022) Salt marsh restoration: an overview of techniques and success indicators. *Environmental Science and Pollution Research* 29:15347–15363
- Boorman L (2003) Saltmarsh Review: An overview of coastal saltmarshes, their dynamic and sensitivity characteristics for conservation and management (JNCC Report No. 334).
- Boorman LA (1999) Salt marshes - present functioning and future change. *Mangroves and Salt Marshes* 3:227–241
- Bouma TJ, van Belzen J, Balke T, Zhu Z, Airoidi L, Blight AJ, Davies AJ, Galvan C, Hawkins SJ, Hoggart SPG, Lara JL, Losada IJ, Maza M, Ondiviela B, Skov MW, Strain EM, Thompson RC, Yang S, Zanuttigh B, Zhang L, Herman PMJ (2014) Identifying knowledge gaps hampering application of intertidal habitats in coastal protection: Opportunities & steps to take. *Coastal Engineering* 87:147–157
- Bouma TJ, De Vries MB, Low E, Kusters L, Herman PMJ, Tańczostańczos IC, Temmerman S, Hesselink A, Meire P, Van Regenmortel & S (2005) Flow hydrodynamics on a mudflat and in salt marsh vegetation: identifying general relationships for habitat characterisations. *Hydrobiologia* 540(1):259-274
- Bouma TJ, De Vries MB, Low E, Peralta G, Tańczos IC, Tańczos T, Van De Koppel J, Herman PMJ (2005) Trade-offs related to ecosystem engineering: a case study on stiffness of emerging macrophytes. *Ecology* 86:2187–2199
- Brown AM, Bass AM, White S, Corr M, Skiba U, MacDonald JM, Pickard AE (2024) The impact of estuarine flushing on greenhouse gases: A study of the stratified Clyde estuary. *Estuarine, Coastal and Shelf Science* 304:108830
- Bruno JF (2000) Facilitation of cobble beach plant communities through habitat modification by *Spartina Alterniflora*. *Ecology* 81:1179–1192
- Brusati ED, Grosholz ED (2006) Native and introduced ecosystem engineers produce contrasting effects on estuarine infaunal communities. *Biological Invasions* 8:683–695
- Carus J, Paul M, Schröder B (2016) Vegetation as self-adaptive coastal protection: Reduction of current velocity and morphologic plasticity of a brackish marsh pioneer. *Ecology and Evolution* 6:1579–1589

- Castagno KA (2018) Salt Marsh Restoration and the Shellfishing Industry: Co-evaluation of Success Components. *Coastal Management* 46:297–315
- Chang CY, Hammitt WE, Chen PK, Machnik L, Su WC (2008) Psychophysiological responses and restorative values of natural environments in Taiwan. *Landscape and Urban Planning* 85:79–84
- Chatagnier J (2012) The biomechanics of salt marsh vegetation applied to wave and surge attenuation. LSU Master's Theses. 1351.
- Chen Y, Thompson C, Collins M (2019) Controls on creek margin stability by the root systems of saltmarsh vegetation, beaulieu estuary, southern england. *Anthropocene Coasts* 2:21–38
- Chmura GL, Anisfeld SC, Cahoon DR, Lynch JC (2003) Global carbon sequestration in tidal, saline wetland soils. *Global Biogeochemical Cycles* 17:1111
- Cooper NJ (2005) Wave Dissipation Across Intertidal Surfaces in the Wash Tidal Inlet, Eastern England. *Journal of Coastal Research* 21:28-40
- Costa MJ, Catarino F, Bettencourt A (2001) The role of salt marshes in the Mira estuary (Portugal). *Wetlands Ecology and Management* 9:121–134
- Costanza R, de Groot R, Sutton P, van der Ploeg S, Anderson SJ, Kubiszewski I, Farber S, Turner RK (2014) Changes in the global value of ecosystem services. *Global Environmental Change* 26:152–158
- Costanza R, Pérez-Maqueo O, Luisa Martinez M, Sutton P, Anderson SJ, Mulder K (2008) The Value of Coastal Wetlands for Hurricane Protection. *Source* 37:241–248
- Cressey M, Johnson M (2004) Report No. 876: Coastal zone assessment survey: Firth of Clyde and Isle of Bute.
- Crooks S, Herr D, Tamelander J, Laffoley D, Vandever J (2011) Marine Ecosystem Series Mitigating Climate Change through Restoration and Management of Coastal Wetlands and Near-shore Marine Ecosystems Challenges and Opportunities.
- Crosby SC, Sax DF, Palmer ME, Booth HS, Deegan LA, Bertness MD, Leslie HM (2016) Salt marsh persistence is threatened by predicted sea-level rise. *Estuarine, Coastal and Shelf Science* 181:93–99
- Deegan LA, Johnson DS, Warren RS, Peterson BJ, Fleeger JW, Fagherazzi S, Wollheim WM (2012) Coastal eutrophication as a driver of salt marsh loss. *Nature* 2012 490:388–392
- Dijkema KS (1987) Geography of the salt marshes in Europe. *Zeitschrift für Geomorphologie* 31:489–499

- Duarte CM, Dennison WC, Orth RJW, Carruthers TJB (2008) The charisma of coastal ecosystems: Addressing the imbalance. *Estuaries and Coasts* 31:233–238
- Fagherazzi S (2014) Storm-proofing with marshes. *Nature Geoscience* 7:701–702
- Fagherazzi S, Mariotti G, Leonardi N, Canestrelli A, Nardin W, Kearney WS (2020) Salt Marsh Dynamics in a Period of Accelerated Sea Level Rise. *Journal of Geophysical Research: Earth Surface* 125:e2019JF005200
- Figueroa-Alfaro RW, van Rooijen A, Garzon JL, Evans M, Harris A (2022) Modelling wave attenuation by saltmarsh using satellite-derived vegetation properties. *Ecological Engineering* 176:106528
- Figurski JD, Malone D, Lacy JR, Denny M (2011) An inexpensive instrument for measuring wave exposure and water velocity: Measuring wave exposure inexpensively. *Limnol. Oceanogr. Meth.* 9:204–214
- Firth CR, Collins PEF (2002) Review No. 108: Coastal processes and management of Scottish Estuaries: IV. Firth of Clyde. Uxbridge
- Foster NM, Hudson MD, Bray S, Nicholls RJ (2013) Intertidal mudflat and saltmarsh conservation and sustainable use in the UK: A review. *Journal of Environmental Management* 126:96–104
- Friedrichs CT, Perry JE (2001) Tidal Wetland Restoration: Physical and Ecological Processes. *Journal of Coastal Research* SI:7-37
- GALLANT (2024) Centre for Sustainable Solutions: GALLANT - Glasgow as a Living Lab Accelerating Novel Transformation.
- Garzon JL, Maza M, Ferreira CM, Lara JL, Losada IJ (2019) Wave Attenuation by *Spartina* Saltmarshes in the Chesapeake Bay Under Storm Surge Conditions. *Journal of Geophysical Research: Oceans* 124:5220–5243
- Gedan KB, Silliman BR, Bertness MD (2009) Centuries of human-driven change in salt marsh ecosystems. *Annual Review of Marine Science* 1:117–141
- Gilby BL, Weinstein MP, Baker R, Cebrian J, Alford SB, Chelsky A, Colombano D, Connolly RM, Currin CA, Feller IC, Frank A, Goeke JA, Goodridge Gaines LA, Hardcastle FE, Henderson CJ, Martin CW, McDonald AE, Morrison BH, Olds AD, Rehage JS, Waltham NJ, Ziegler SL (2021) Human Actions Alter Tidal Marsh Seascapes and the Provision of Ecosystem Services. *Estuaries and Coasts* 44:1628–1636
- Giuliani S, Bellucci LG (2019) Salt Marshes: Their Role in Our Society and Threats Posed to Their Existence. *World Seas: An Environmental Evaluation Volume III: Ecological Issues and Environmental Impacts* 79–101

- Gramling R, Hagelman R (2005) Strategies for Restoration of Louisiana's Coastal Wetlands and Barrier Islands. *Journal of Coastal Research* 21:112–133
- Gu J, Luo M, Zhang X, Christakos G, Agusti S, Duarte CM, Wu J (2018) Losses of salt marsh in China: Trends, threats and management. *Estuarine, Coastal and Shelf Science* 214:98–109
- Hansen AB, Carstensen S, Christensen DF, Aagaard T (2017) Performance Of A Tilt Current Meter In The Surf Zone. *Coast. Dynam.* 218:944–954
- Hansom J, Maxwell F, Naylor L, Piedra M (2017) SNH Commissioned Report No. 891: Impacts of sea-level rise and storm surges due to climate change in the Firth of Clyde.
- Harley CDG, Bertness MD (1996) Structural Interdependence: An Ecological Consequence of Morphological Responses to Crowding in Marsh Plants. *Ecology* 77:654–661
- Hasibuan IM, Amelia R, Bimantara Y, Susetya IE, Susilowati A, Basyuni M (2021) Vegetation and macrozoobenthos diversity in the Percut Sei Tuan mangrove forest, North Sumatra, Indonesia. *Biodiversitas Journal of Biological Diversity* 22:5600–5608
- Haynes TA (2016) SNH Commissioned Report 786: Scottish saltmarsh survey national report.
- Hermes J, Albert C, von Haaren C (2018) Assessing the aesthetic quality of landscapes in Germany. *Ecosystem Services* 31:296–307
- Himes-Cornell A, Pendleton L, Atiyah P (2018) Valuing ecosystem services from blue forests: A systematic review of the valuation of salt marshes, sea grass beds and mangrove forests. *Ecosystem Services* 30:36–48
- Le Hir P, Roberts W, Cazaillet O, Christie M, Bassoullet P, Bacher C (2000) Characterization of intertidal flat hydrodynamics. *Continental Shelf Research* 20:1433–1459
- Hughes RG (2004) Climate change and loss of saltmarshes: Consequences for birds. *Ibis* 146:21–28
- Inverclyde Council (2019) Natural Heritage Designations.
- James P. M. Syvitski, Kettner AJ, Overeem I, Hutton EWH, Hannon MT, Brakenridge GR, Day J, Vörösmarty C, Saito Y, Giosan L, Nicholls RJ (2009) Sinking deltas due to human activities. *Nature Geoscience* 2:681–686
- Jones G, Ahmed S (2000) The impact of coastal flooding on conservation areas: A study of the Clyde Estuary, Scotland. *Journal of Coastal Conservation* 171–180
- Karunarathna H (2011) Modelling the long-term morphological evolution of the Clyde Estuary, Scotland, UK. *Journal of Coastal Conservation* 15:499–507

- Kaya Y, Stewart M, Becker M (2005) Flood Forecasting and Flood Warning in the Firth of Clyde, UK. *Natural Hazards* 257–271
- Keimer K, Kosmalla V, Prüter I, Lojek O, Prinz M, Schürenkamp D, Freund H, Goseberg N (2023) Proposing a novel classification of growth periods based on biomechanical properties and seasonal changes of *Spartina anglica*. *Frontiers in Marine Science* 10:1095200
- Kirwan ML, Guntenspergen GR (2010) Influence of tidal range on the stability of coastal marshland. *Journal of Geophysical Research: Earth Surface* 115:2009
- Kirwan ML, Guntenspergen GR, D’Alpaos A, Morris JT, Mudd SM, Temmerman S (2010) Limits on the adaptability of coastal marshes to rising sea level. *Geophysical Research Letters* 37:23401
- Kirwan ML, Temmerman S, Skeeahan EE, Guntenspergen GR, Fagherazzi S (2016) Overestimation of marsh vulnerability to sea level rise. *Nature Climate Change* 2016 6:3 6:253–260
- Kiviat E, Hamilton E (2001) *Phragmites* use by Native North Americans. *Aquatic Botany* 69:341–357
- Knottnerus OS (2005) History of human settlement, cultural change and interference with the marine environment. *Helgoland Marine Research* 59:2–8
- Köbbing JF, Thevs N, Zerbe S (2013) The utilisation of reed (*Phragmites australis*): a review. *Mires and Peat* 13:1–14
- Ladd CJT, Vovides AG, Wimmmler M-C, Schwarz C, Balke T (2024) The Mini Buoy Handbook: Assessing hydrodynamics in intertidal environments.
- Ladd CJT, Duggan-Edwards MF, Pagès JF, Skov MW (2021) Saltmarsh Resilience to Periodic Shifts in Tidal Channels. *Frontiers in Marine Science* 8:757715
- Ladd CJT, Vovides AG, Wimmmler MC, Schwarz C, Balke T (2024) Monitoring tides, currents, and waves along coastal habitats using the Mini Buoy. *Limnology and Oceanography: Methods* 25:1229–1244
- Leonard LA, Croft AL (2006) The effect of standing biomass on flow velocity and turbulence in *Spartina alterniflora* canopies. *Estuarine, Coastal and Shelf Science* 69:325–336
- Leonard LA, Luther ME (1995) Flow hydrodynamics in tidal marsh canopies. *Limnology and Oceanography* 40:1474–1484
- Leonardi N, Carnacina I, Donatelli C, Ganju NK, Plater AJ, Schuerch M, Temmerman S (2018) Dynamic interactions between coastal storms and salt marshes: A review. *Geomorphology* 301:92–107

- Da Lio C, D'Alpaos A, Marani M (2013) The secret gardener: Vegetation and the emergence of biogeomorphic patterns in tidal environments. *Philosophical Transactions of the Royal Society A: Mathematical, Physical and Engineering Sciences* 371
- Da Lio C, Teatini P, Strozzi T, Tosi L (2018) Understanding land subsidence in salt marshes of the Venice Lagoon from SAR Interferometry and ground-based investigations. *Remote Sensing of Environment* 205:56–70
- Lotze HK, Lenihan HS, Bourque BJ, Bradbury RH, Cooke RG, Kay MC, Kidwell SM, Kirby MX, Peterson CH, Jackson JBC (2006) Depletion, Degradation, and Recovery Potential of Estuaries and Coastal Seas. *Science* 312:1806–1809
- Maniatis, G (2021) On the use of IMU (inertial measurement unit) sensors in geomorphology. *Earth Surf. Process. Landforms* 46:2136–2140
- Marani M, Silvestri S, Belluco E, Ursino N, Comerlati A, Tosatto O, Putti M (2006) Spatial organization and ecohydrological interactions in oxygen-limited vegetation ecosystems. *Water Resources Research* 42:W06D06
- McGranahan G, Balk D, Anderson B (2007) The rising tide: assessing the risks of climate change and human settlements in low elevation coastal zones. *Environment and Urbanization* 19:17
- McKinley E, Pagès JF, Alexander M, Burdon D, Martino S (2020) Uses and management of saltmarshes: A global survey. *Estuarine, Coastal and Shelf Science* 243:106840
- Mcowen CJ, Weatherdon L V., Van Bochove JW, Sullivan E, Blyth S, Zockler C, Stanwell-Smith D, Kingston N, Martin CS, Spalding M, Fletcher S (2017) A global map of saltmarshes. *Biodiversity Data Journal* 5:e11764
- Mendez FJ, Losada IJ (2004) An empirical model to estimate the propagation of random breaking and nonbreaking waves over vegetation fields. *Coastal Engineering* 51:103–118
- Möller I (2006) Quantifying saltmarsh vegetation and its effect on wave height dissipation: Results from a UK East coast saltmarsh. *Estuarine, Coastal and Shelf Science* 69:337–351
- Möller I, Kudella M, Rupprecht F, Spencer T, Paul M, Van Wesenbeeck BK, Wolters G, Jensen K, Bouma TJ, Miranda-Lange M, Schimmels S (2014) Wave attenuation over coastal salt marshes under storm surge conditions. *Nature Geoscience* 2014 7:107:727–731

- Möller I, Spencer T (2002) Wave dissipation over macro-tidal saltmarshes: Effects of marsh edge typology and vegetation change. In: Journal of Coastal Research.Vol. 36 Coastal Education Research Foundation Inc. pp. 506–521.
- Möller I, Spencer T, French JR, Leggett DJ, Dixon M (1999) Wave Transformation Over Salt Marshes: A Field and Numerical Modelling Study from North Norfolk, England. Estuarine, Coastal and Shelf Science 49:411–426
- Möller IBA, Spencer T, French JR, Leggett DJ, Dixon M (2001) The sea-defence value of salt marshes: Field evidence from north Norfolk. Water and Environment Journal 15:109–116
- Morris JT (2006) Competition among marsh macrophytes by means of geomorphological displacement in the intertidal zone. Estuarine, Coastal and Shelf Science 69:395– 402
- Moser SC, Jeffress Williams S, Boesch DF (2012) Wicked challenges at land's end: Managing coastal vulnerability under climate change. Annual Review of Environment and Resources 37:51–78
- Mueller P, Ladiges N, Jack A, Schmiedl G, Kutzbach L, Jensen K, Nolte S (2019) Assessing the long-term carbon-sequestration potential of the semi-natural salt marshes in the European Wadden Sea. Ecosphere 10:e02556
- Murray NJ, Worthington TA, Bunting P, Duce S, Hagger V, Lovelock CE, Lucas R, Saunders MI, Sheaves M, Spalding M, Waltham NJ, Lyons MB (2022) High-resolution mapping of losses and gains of Earth's tidal wetlands. Science 376:744–749
- Neumeier U, Amos CL (2006) The influence of vegetation on turbulence and flow velocities in European salt-marshes. Sedimentology 53:259–277
- Neumeier U, Ciavola P (2004) Flow Resistance and Associated Sedimentary Processes in a *Spartina maritima* Salt-Marsh. Journal of Coastal Research 20:435–447
- Newton A, Icely J, Cristina S, Perillo GME, Turner RE, Ashan D, Cragg S, Luo Y, Tu C, Li Y, Zhang H, Ramesh R, Forbes DL, Solidoro C, Béjaoui B, Gao S, Pastres R, Kelsey H, Taillie D, Nhan N, Brito AC, de Lima R, Kuenzer C (2020) Anthropogenic, Direct Pressures on Coastal Wetlands. Frontiers in Ecology and Evolution 8:512636
- Otto FEL, Van Der Wiel K, Van Oldenborgh GJ, Philip S, Kew SF, Uhe P, Cullen H (2018) Climate change increases the probability of heavy rains in Northern England/Southern Scotland like those of storm Desmond - A real-time event attribution revisited. Environmental Research Letters 13:024006
- Pannoizzo N, Leonardi N, Carnacina I, Smedley R (2021) Salt marsh resilience to sea-level rise and increased storm intensity. Geomorphology 389:107825

- Pétillon J, McKinley E, Alexander M, Adams JB, Angelini C, Balke T, Griffin JN, Bouma T, Hacker S, He Q, Hensel MJS, Ibáñez C, Macreadie PI, Martino S, Sharps E, Ballinger R, de Battisti D, Beaumont N, Burdon D, Daleo P, D'Alpaos A, Duggan-Edwards M, Garbutt A, Jenkins S, Ladd CJT, Lewis H, Mariotti G, McDermott O, Mills R, Möller I, Nolte S, Pagès JF, Silliman B, Zhang L, Skov MW (2023) Top ten priorities for global saltmarsh restoration, conservation and ecosystem service research. *Science of the Total Environment* 898:165544
- Puijalon S, Bornette G, Sagnes P (2005) Adaptations to increasing hydraulic stress: Morphology, hydrodynamics and fitness of two higher aquatic plant species. *Journal of Experimental Botany* 56:777–786
- Puijalon S, Léna JP, Rivière N, Champagne JY, Rostan JC, Bornette G (2008) Phenotypic plasticity in response to mechanical stress: Hydrodynamic performance and fitness of four aquatic plant species. *New Phytologist* 177:907–917
- Rendón OR, Garbutt A, Skov M, Möller I, Alexander M, Ballinger R, Wyles K, Smith G, McKinley E, Griffin J, Thomas M, Davidson K, Pagès JF, Read S, Beaumont N (2019) A framework linking ecosystem services and human well-being: Saltmarsh as a case study. *People and Nature* 1:486–496
- Rennie AF, Hansom JD (2011) Sea level trend reversal: Land uplift outpaced by sea level rise on Scotland's coast. *Geomorphology* 125:193–202
- Resio DT, Westerink JJ (2008) Modeling the physics of storm surges. *Physics Today* 61:33-38
- Ríos S, Obón C, Martínez-Francés V, Verde A, Ariza D, Laguna E (2020) Halophytes as Food. In: *Handbook of Halophytes*. Springer International Publishing, Cham pp. 1–36.
- Rogers K, Wilton KM, Saintilan N (2006) Vegetation change and surface elevation dynamics in estuarine wetlands of southeast Australia. *Estuarine, Coastal and Shelf Science* 66:559–569
- Rupp-Armstrong S, Nicholls RJ (2007) Coastal and estuarine retreat: A comparison of the application of managed realignment in England and Germany. *Journal of Coastal Research* 23:1418–1430
- Rupprecht F, Möller I, Paul M, Kudella M, Spencer T, van Wesenbeeck BK, Wolters G, Jensen K, Bouma TJ, Miranda-Lange M, Schimmels S (2017) Vegetation-wave interactions in salt marshes under storm surge conditions. *Ecological Engineering* 100:301–315



- Saintilan N, Wilson NC, Rogers K, Rajkaran A, Krauss KW (2014) Mangrove expansion and salt marsh decline at mangrove poleward limits. *Global Change Biology* 20:147–157
- Schuerch M, Vafeidis A, Slawig T, Temmerman S (2013) Modeling the influence of changing storm patterns on the ability of a salt marsh to keep pace with sea level rise. *Journal of Geophysical Research: Earth Surface* 118:84–96
- Schulze D, Rupprecht F, Nolte S, Jensen K (2019) Seasonal and spatial within-marsh differences of biophysical plant properties: implications for wave attenuation capacity of salt marshes. *Aquatic Sciences* 81:1–11
- Shao D, Zhou W, Bouma TJ, Asaeda T, Wang ZB, Liu X, Sun T, Cui B (2020) Physiological and biochemical responses of the salt-marsh plant *Spartina alterniflora* to long-term wave exposure. *Annals of Botany* 125:291–299
- Sheng YP, Lapetina A, Ma G (2012) The reduction of storm surge by vegetation canopies: Three-dimensional simulations. *Geophysical Research Letters* 39
- Silinski A, Schoutens K, Puijalon S, Schoelynck J, Luyckx D, Troch P, Meire P, Temmerman S (2018) Coping with waves: Plasticity in tidal marsh plants as self-adapting coastal ecosystem engineers. *Limnology and Oceanography* 63:799–815
- Smolders S, Plancke Y, Ides S, Meire P, Temmerman S (2015) Role of intertidal wetlands for tidal and storm tide attenuation along a confined estuary: a model study. *Nat. Hazards Earth Syst. Sci.* 15:1659–1675
- Sousa AI, Lillebø AI, Pardal MA, Caçador I (2010) Productivity and nutrient cycling in salt marshes: Contribution to ecosystem health. *Estuarine, Coastal and Shelf Science* 87:640–646
- Spalding MD, Mcivor AL, Beck MW, Koch EW, Möller I, Reed DJ, Rubinoff P, Spencer T, Tolhurst TJ, Wamsley T V., van Wesenbeeck BK, Wolanski E, Woodroffe CD (2014) Coastal ecosystems: A critical element of risk reduction. *Conservation Letters* 7:293–301
- Stark J, Plancke Y, Ides S, Meire P, Temmerman S (2016) Coastal flood protection by a combined nature-based and engineering approach: Modeling the effects of marsh geometry and surrounding dikes. *Estuarine, Coastal and Shelf Science* 175:34–45
- Sutton-Grier AE, Wowk K, Bamford H (2015) Future of our coasts: The potential for natural and hybrid infrastructure to enhance the resilience of our coastal communities, economies and ecosystems. *Environmental Science and Policy* 51:137–148
- Taubert RB, Murphy KJ (2012) Long-term dynamics in Scottish saltmarsh plant communities. *Glasgow Naturalist* 25:111-118

- Temmerman S, Meire P, Bouma TJ, Herman PMJ, Ysebaert T, De Vriend HJ (2013) Ecosystem-based coastal defence in the face of global change. *Nature* 504:79–83
- Temmerman S, De Vries MB, Bouma TJ (2012) Coastal marsh die-off and reduced attenuation of coastal floods: A model analysis. *Global and Planetary Change* 92–93:267–274
- Torio DD, Chmura GL (2013) Assessing Coastal Squeeze of Tidal Wetlands. *Journal of Coastal Research* 29:1049–1061
- Townend I, Fletcher C, Knappen M, Rossington K (2011) A review of salt marsh dynamics. *Water and Environment Journal* 25:477–488
- UNEP (2006) Marine and coastal ecosystems and human well-being: A synthesis report based on the findings of the Millennium Ecosystem Assessment.
- Vovides AG, Vogt J, Kollert A, Berger U, Grueters U, Peters R, Lara-Domínguez AL, López-Portillo J (2014) Morphological plasticity in mangrove trees: salinity-related changes in the allometry of *Avicennia germinans*. *Trees - Structure and Function* 28:1413–1425
- van der Wal D, Pye K (2004) Patterns, rates and possible causes of saltmarsh erosion in the Greater Thames area (UK). *Geomorphology* 61:373–391
- Waltham NJ, Elliott M, Lee SY, Lovelock C, Duarte CM, Buelow C, Simenstad C, Nagelkerken I, Claassens L, Wen CKC, Barletta M, Connolly RM, Gillies C, Mitsch WJ, Ogburn MB, Purandare J, Possingham H, Sheaves M (2020) UN Decade on Ecosystem Restoration 2021–2030—What Chance for Success in Restoring Coastal Ecosystems? *Frontiers in Marine Science* 7:518980
- Wamsley T V., Cialone MA, Smith JM, Atkinson JH, Rosati JD (2010) The potential of wetlands in reducing storm surge. *Ocean Engineering* 37:59–68
- Wamsley T V., Cialone MA, Smith JM, Ebersole BA, Grzegorzewski AS (2009) Influence of landscape restoration and degradation on storm surge and waves in southern Louisiana. *Natural Hazards* 51:207–224
- Weston NB (2014) Declining Sediments and Rising Seas: An Unfortunate Convergence for Tidal Wetlands. *Estuaries and Coasts* 37:1–23
- Whitfield AK (2017) The role of seagrass meadows, mangrove forests, salt marshes and reed beds as nursery areas and food sources for fishes in estuaries. *Reviews in Fish Biology and Fisheries* 2016 27:1 27:75–110
- Wong PP, Losada I, Gattuso J, Hinkel J, Khattabi A, Mcinnes K, Saito Y, Sallenger A (2014) Coastal Systems and Low-Lying Areas. In: *Climate Change 2014: Impacts, Adaptation, and Vulnerability. Part A: Global and Sectoral Aspects. Contribution of*

Working Group II to the Fifth Assessment Report of the Intergovernmental Panel on Climate Change. Field, CB, Barros, VR, Dokken, DJ, K.J. Mach, KJ, Mastrandrea, MD, Bilir, TE, Chatterjee, M, Ebi, KL, Estrada, YO, Genova, RC, Girma, B, Kissel, ES, Levy, AN, MacCracken, S, Mastrandrea, PR, & White, LL, editors. Cambridge University Press, Cambridge, United Kingdom and New York, NY, USA pp. 361–409.

World Population Review (2024) World Population Review.

Xu Y, Esposito CR, Beltrán-Burgos M, Nepf HM (2022) Competing effects of vegetation density on sedimentation in deltaic marshes. *Nature Communications* 13:4641

Yang SL, Li H, Ysebaert T, Bouma TJ, Zhang WX, Wang YY, Li P, Li M, Ding PX (2008) Spatial and temporal variations in sediment grain size in tidal wetlands, Yangtze Delta: On the role of physical and biotic controls. *Estuarine, Coastal and Shelf Science* 77:657–671

Yang SL, Shi BW, Bouma TJ, Ysebaert T, Luo XX (2012) Wave Attenuation at a Salt Marsh Margin: A Case Study of an Exposed Coast on the Yangtze Estuary. *Estuaries and Coasts* 35:169–182

Ysebaert T, Yang SL, Zhang L, He Q, Bouma TJ, Herman PMJ (2011) Wave attenuation by two contrasting ecosystem engineering salt marsh macrophytes in the intertidal pioneer zone. *Wetlands* 31:1043–1054

Zedler JB, Kercher S (2004) Causes and Consequences of Invasive Plants in Wetlands: Opportunities, Opportunists, and Outcomes. *Critical Reviews in Plant Sciences* 23:431–452

Zoderer BM, Tasser E, Carver S, Tappeiner U (2019) Stakeholder perspectives on ecosystem service supply and ecosystem service demand bundles. *Ecosystem Services* 37:100938